

1 **Producing distribution maps for informing ecosystem-based fisheries management**
2 **using a comprehensive survey database and spatio-temporal models**

3
4 **Arnaud Grüss^{1*}, James T. Thorson², Elizabeth A. Babcock¹ and Joseph H. Tarnecki³**

5
6 ¹Department of Marine Biology and Ecology, Rosenstiel School of Marine and
7 Atmospheric Science, University of Miami, 4600 Rickenbacker Causeway, Miami, FL,
8 33149, USA

9
10 ²Fisheries Resource Assessment and Monitoring Division (FRAM), Northwest Fisheries
11 Science Center, National Marine Fisheries Service (NMFS), NOAA, 2725, Montlake
12 Boulevard E, Seattle, WA 98112, USA

13
14 ³Florida Fish and Wildlife Conservation Commission, Fish and Wildlife Research Institute,
15 100 8th Ave SE, St. Petersburg, FL 33701, USA

16
17 ***Type of article:*** Original article

18
19 ***Manuscript length***

20 Abstract (299 words), Core text (6,651 words), References (60)

21 7 figures, 4 tables, 1 box

22 4 figures, 3 tables and 2 appendices appearing in the Supplementary material.

23
24 **** Corresponding author***

25 Dr. Arnaud Grüss

26 Department of Marine Biology and Ecology

27 Rosenstiel School of Marine and Atmospheric Science, University of Miami

28 4600 Rickenbacker Causeway

29 Miami, FL, 33149

30 United States of America

31 Telephone: (01) 305 421 4262

32 Email: agruss@rsmas.miami.edu

33 **ABSTRACT**

34 Ecosystem-based fisheries-management (EBFM) is increasingly used in the United
35 States (U.S.), including in the Gulf of Mexico (GOM). Producing distribution maps for
36 marine organisms is a critical step in the implementation of EBFM. In particular,
37 distribution maps are important inputs for many spatially-explicit ecosystem models, such
38 as OSMOSE models, as well as for biophysical models used to predict annual recruitment
39 anomalies due to oceanographic factors. In this study, we applied a recently proposed
40 statistical modelling framework to produce distribution maps for: (1) younger juveniles
41 (ages 0-1) of red snapper (*Lutjanus campechanus*), red grouper (*Epinephelus morio*) and
42 gag (*Mycteroperca microlepis*), so as to be able to define the potential larval settlement
43 areas of the three species in a biophysical model; and (2) the functional groups and life
44 stages represented in the OSMOSE model of the West Florida Shelf (“OSMOSE-WFS”).
45 This statistical modelling framework consists of: (1) compiling a large database blending
46 all of the encounter/non-encounter data of the GOM collected by the fisheries-independent
47 and fisheries-dependent surveys using random sampling schemes, referred to as the
48 “comprehensive survey database”; (2) employing the comprehensive survey database to fit
49 spatio-temporal binomial generalized linear mixed models (GLMMs) that integrate the
50 confounding effects of survey and year; and (3) using the predictions of the fitted spatio-
51 temporal binomial GLMMs to generate distribution maps. This large endeavour allowed us
52 to produce distribution maps for younger juveniles of red snapper, red grouper and gag and
53 nearly all of the other functional groups and life stages represented in OSMOSE-WFS, at
54 different seasons. Using Pearson residuals, the probabilities of encounter predicted by all
55 spatio-temporal binomial GLMMs were demonstrated to be reasonable. Moreover, the
56 results obtained for younger juvenile fish concur with the literature, provide additional

57 insights into the spatial distribution patterns of these life stages, and highlight important
58 future research avenues.

59

60 **Key words:** distribution maps; ecosystem-based fisheries management (EBFM); spatially-
61 explicit ecosystem models; biophysical models; comprehensive survey database;
62 generalized linear mixed models (GLMMs)

63 **Introduction**

64 Ecosystem-based fisheries-management (EBFM) is increasingly being used in the
65 United States (U.S.), including in the Gulf of Mexico (GOM) (Levin *et al.*, 2014;
66 Samhouri *et al.*, 2014; Grüss *et al.*, 2017a; Harvey *et al.*, 2017). Producing distribution
67 maps for marine organisms is a critical step in the implementation of EBFM (Mace *et al.*,
68 2001; MSFCMA, 2007). In particular, distribution maps are important inputs for a number
69 of spatially-explicit ecosystem models, such as applications of the OSMOSE (Shin and
70 Cury, 2001, 2004) and Atlantis (Fulton *et al.*, 2004, 2011) modelling platforms, as well as
71 for biophysical models used to predict annual recruitment anomalies due to oceanographic
72 factors, such as the Connectivity Modelling System (CMS; Paris *et al.*, 2013). In
73 ecosystem models, distribution maps and simulated movement patterns (e.g., seasonal
74 migrations) are used to allocate the biomasses of modelled marine organisms over space;
75 in this way, distribution maps influence patterns of spatial overlap between functional
76 groups and, consequently, trophic interactions between these functional groups (Grüss *et*
77 *al.*, 2016a). In biophysical models such as the CMS, distribution maps are needed to define
78 spatial patterns of egg production and the potential larval settlement areas of the species
79 under consideration (Karnauskas *et al.*, 2013a, 2013b; Grüss *et al.*, 2014b).

80 The production of distribution maps for spatially-explicit ecosystem and
81 biophysical models has generally relied on simplistic methodologies (Grüss *et al.*, 2016a).
82 Two exceptions to this general pattern are the methodologies developed by Drexler and
83 Ainsworth (2013) for the Atlantis model of the GOM (“Atlantis-GOM”) and Grüss *et al.*
84 (2014a) for the OSMOSE model of the West Florida Shelf (“OSMOSE-WFS”). Drexler
85 and Ainsworth (2013) generated distribution maps for Atlantis-GOM from the predictions
86 of negative binomial generalized additive models (GAMs) fitted to a groundfish trawl
87 survey dataset. Grüss *et al.* (2014) produced distribution maps for OSMOSE-WFS using

88 the predictions of delta GAMs fitted to a groundfish trawl, a video, or a bottom longline
89 survey dataset. While Drexler and Ainsworth (2013) and Grüss *et al.* (2014a)'s
90 methodologies represent improvements over previous methodologies for generating
91 distribution maps for spatially-explicit ecosystem models, they also have limitations. First,
92 Drexler and Ainsworth (2013) and Grüss *et al.* (2014a) relied on a limited amount of
93 survey data for some functional groups, which led in some cases to unreliable predictions
94 of spatial distributions. Then, Drexler and Ainsworth (2013) and Grüss *et al.* (2014a)
95 employed survey data that were not appropriate in some cases (e.g., groundfish trawl
96 survey data for some pelagic functional groups). Finally, Drexler and Ainsworth (2013)
97 and Grüss *et al.* (2014a)'s approaches were not geospatial and, therefore, resulted in
98 substantial, unmodelled spatial patterns in GAM residuals for many functional groups.

99 Grüss *et al.* (2016a) proposed a novel statistical modelling framework that
100 addresses the limitations of Drexler and Ainsworth (2013) and Grüss *et al.* (2014a)'s
101 methodologies. Grüss *et al.* (2016a)'s proposed statistical modelling framework consists
102 of: (1) compiling a large database blending all of the encounter/non-encounter data of the
103 U.S. GOM collected by the fisheries-independent and fisheries-dependent surveys that use
104 random sampling schemes (i.e., that do not use fixed-station designs or do not compile
105 fisheries catch time series for specific areas of the GOM), referred to as the
106 “comprehensive survey database”; (2) employing the comprehensive survey database to fit
107 binomial statistical models that integrate the confounding effects of “gear” (where each
108 gear type specifies a survey dataset) and year; and (3) using the predictions of the fitted
109 binomial statistical models to produce distribution maps for the U.S. GOM. Grüss *et al.*
110 (2016a)'s methodology is particularly appropriate for generating distribution maps for
111 groupers (Epinephelidae), as demonstrated in a previous study (Grüss *et al.*, 2017b). In
112 Grüss *et al.* (2017b), spatio-temporal binomial generalized linear mixed models (GLMMs)

113 were developed, using a blending of encounter/non-encounter data for red grouper
114 (*Epinephelus morio*) and gag (*Mycteroperca microlepis*) collected by six fisheries-
115 independent and three fisheries-dependent surveys of the U.S. GOM. Then, the predictions
116 of fitted spatio-temporal binomial GLMMs were employed to generate probability of
117 encounter maps for the older juvenile (ages 1 – 3) and adult (ages 3+) stages of red grouper
118 and gag. Grüss *et al.* (2017b) showed that the predictions of their spatio-temporal binomial
119 GLMMs were reasonable. Yet, the authors found that, in the case of adult gag, observed
120 frequency of encounter for samples with highest predicted encounter probability was
121 considerably smaller than the estimated 95% confidence interval for these samples; this
122 result was attributed to the relatively limited amount of data available to the authors for
123 adult gag, which yielded low observed frequency of encounter for the highest probability
124 samples.

125 In the present study, we apply Grüss *et al.* (2016a)'s statistical modelling
126 framework to produce distribution maps for: (1) the younger juveniles (ages 0-1) of red
127 snapper (<22.9 cm TL), red grouper (<14.8 cm TL) and gag (<20 cm TL), so as to
128 delineate the potential larval settlement areas of the three species in the CMS biophysical
129 model; and (2) the functional groups represented in the OSMOSE-WFS ecosystem model.
130 All these distribution maps were generated using the predictions of spatio-temporal
131 binomial GLMMs fitted to the comprehensive survey database that we compiled for the
132 U.S. GOM (hereafter often simply referred to as "GOM"). First, we report the
133 development of the comprehensive survey database, which gathered a sufficient amount of
134 encounter/non-encounter data coming from 37 different survey datasets to generate
135 distribution maps for the younger juveniles of red snapper, red grouper and gag, and nearly
136 all of the functional groups represented in OSMOSE-WFS. Then, we produce and evaluate
137 distribution maps, with a focus on younger juveniles of red snapper, red grouper and gag.

138 Finally, we use these distribution maps to estimate the percentages of spatial overlap
139 between younger juveniles of red snapper, red grouper and gag and the older juvenile and
140 adult stages of red grouper and gag in the West Florida Shelf region, so as to revisit a
141 contentious result of the latest published versions of OSMOSE-WFS (Grüss *et al.*, 2016b,
142 2016c).

143

144 **Material and methods**

145 *Study areas*

146 The GOM is a Large Marine Ecosystem bordered by the U.S., Mexico and Cuba
147 (NOS, 2008). The U.S. GOM is bounded on the east by the West Florida Shelf, on the
148 north by the states of Mississippi, Alabama and Louisiana, and on the west by the state of
149 Texas. The area of the West Florida Shelf considered in the OSMOSE-WFS model
150 excludes the Florida Keys and Dry Tortugas (Figures 1 and 2a).

151

152 *Study functional groups, species and life stages*

153 *Younger juveniles of red snapper, red grouper and gag*

154 Red snapper, red grouper and gag are demersal fish characterized by small home
155 ranges and high site fidelity (Bullock and Smith, 1991; Workman *et al.*, 2002; Coleman *et*
156 *al.*, 2010, 2011). The three species undertake several ontogenetic migrations during their
157 life cycle (Mullaney Jr, 1994; Gallaway *et al.*, 2009; Saul *et al.*, 2012; Carruthers *et al.*,
158 2015). The first of these ontogenetic migrations occurs when fish reach age 1 (i.e., when
159 they transition from the younger juvenile to the older juvenile stage). At around one year of
160 age, red snapper migrates to deeper, higher-relief areas (Szedlmayer and Conti, 1999;
161 Gallaway *et al.*, 2009), while red grouper and gag migrate from nearshore shallow areas to
162 inshore reefs (Koenig and Coleman, 1998; Switzer *et al.*, 2012).

163 The habitats of younger juveniles of red snapper, red grouper and gag differ.
164 Younger juvenile red snappers are distributed over low-relief areas, characterized by
165 patches of rubble, debris, or relic shell beds associated with sand and mud (Szedlmayer and
166 Conti, 1999; Gallaway *et al.*, 2009). Younger juvenile red groupers do not require specific
167 habitats; they are found in estuaries, in inshore hard bottom areas and on seagrass beds
168 (Moe, 1969; Koenig and Coleman, 1999; Coleman *et al.*, 2010). By contrast, younger
169 juvenile gags are dependent on high-salinity estuaries (Koenig and Coleman, 1998;
170 Fitzhugh *et al.*, 2005; Switzer *et al.*, 2012), where they inhabit primarily seagrass beds, but
171 also mangroves, oyster reefs, jetties and seawalls (Hastings, 1979; Bullock and Smith,
172 1991; Koenig and Coleman, 1998, 1999; Casey *et al.*, 2007). Recently, Ingram *et al.*
173 (2013) combined three fisheries-independent databases to produce abundance indices for
174 younger juvenile gag for the eight regions of the GOM where the life stage is consistently
175 found: (1) Saint Andrew Bay; (2) Saint Joe Bay; (3) Turkey Point; (4) the Mid Big Bend;
176 (5) Cedar Key; (6) Tampa Bay; (7) Sarasota Bay; and (8) Charlotte Harbor (Figure 2b).

177

178 *Functional groups of the OSMOSE-WFS model*

179 OSMOSE is a spatially-explicit individual-based, multispecies modelling approach,
180 which simulates the entire life cycle of several (typically 10-15) high trophic level (HTL)
181 functional groups and is forced by fields of biomass for low trophic level (LTL) functional
182 groups (Shin and Cury, 2001, 2004 ; Grüss *et al.*, 2016b). Distribution maps are provided
183 to OSMOSE at each modelled time step to allocate the biomasses of HTL and LTL groups
184 over space. When the distribution of a given HTL functional group or of a given life stage
185 of a HTL functional group remains static during seasonal or yearly time frames, the
186 individuals of this functional group or life stage move to model cells immediately adjacent
187 to their current cell according to a random walk. In OSMOSE, a parameter determines the

188 range of random walk movements of HTL functional groups and life stages and, therefore,
189 can account for the fact that some HTL functional groups and life stages have lower site
190 fidelity than others; however, this parameter is usually set to its default value of 1.0 cell
191 (but see Halouani *et al.*, 2016). Contrary to most ecosystem modeling platforms, OSMOSE
192 does not use a diet matrix, but rather makes the assumption that predation is an
193 opportunistic process and that a predator will feed on any prey item if: (1) the predator and
194 the potential prey overlap over space, as determined by distribution maps defined for
195 specific functional groups, life stages and seasons; (2) there is size adequacy between the
196 predator and the potential prey, as determined by “predator/prey size ratios”; and, (3) the
197 potential prey is accessible to the predator, in relation to its vertical distribution and
198 morphology, as determined by “accessibility coefficients” (Grüss *et al.*, 2016b; Fu *et al.*,
199 2017). OSMOSE is a stochastic modelling approach, because it: (1) uses distribution maps
200 to distribute only a limited number of HTL individuals over space at run time; (2)
201 implements random walk movement when the distribution of HTL individuals remains
202 static; and (3) employs a stochastic mortality algorithm to compute the mortality rates of
203 HTL functional groups (Grüss *et al.*, 2016b).

204 OSMOSE-WFS is an application of the OSMOSE modelling approach with a
205 spatial resolution of 0.18° and a monthly time step, which describes the trophic structure of
206 the West Florida Shelf ecosystem in the 2000s (Figure 2a). Three versions of OSMOSE-
207 WFS have been developed and undergone validation (Grüss *et al.*, 2015, 2016b, 2016c).
208 Twelve HTL fish and invertebrate functional groups are represented in OSMOSE-WFS.
209 The model is forced by biomass fields for seven LTL functional groups, consisting of
210 phytoplankton, zooplankton, and five LTL benthic groups (Figure 3). The designation of
211 functional groups as either HTL or LTL groups in OSMOSE-WFS was based on the food
212 web structure described in another ecosystem model of the West Florida Shelf (“WFS Reef

213 fish Ecopath”; Chagaris, 2013). The OSMOSE-WFS functional groups considered in this
214 study include the twelve HTL functional groups and the five LTL benthic groups (Table
215 1).

216 Some of the HTL functional groups represented in OSMOSE-WFS are made of
217 only one species of high economic importance. This is the case for the “red snapper”, “red
218 grouper” and “gag” functional groups.

219

220 ***Compilation of a comprehensive survey database for the GOM***

221 We requested data for the period of 2000-2016 from the different federal and state
222 agencies, universities and non-governmental organizations that either collect survey data in
223 the GOM using random sampling schemes, or randomly sample fisheries operations in the
224 GOM with observer programs. We received a total of 37 different datasets, including 29
225 fisheries-independent and eight fisheries-dependent datasets (Table 2 and Supplementary
226 Table S1).

227 We conducted a literature review to determine: (1) for which life stages of the HTL
228 functional groups represented in OSMOSE-WFS we should produce distribution maps; and
229 (2) whether we should produce annual or seasonal maps for the different HTL functional
230 groups/life stages and LTL functional groups represented in OSMOSE-WFS
231 (Supplementary Table S2). It was necessary to generate distribution maps for different life
232 stages of a given HTL functional group when the literature review revealed that this
233 functional group undertakes ontogenetic migrations, i.e., changes habitats as it grows older
234 (e.g., red snapper; Gallaway *et al.*, 2009).

235 Next, we extracted the following information from each of the 37 survey datasets
236 for each functional group/life stage: (1) the latitudes and longitudes at which the sampling
237 events took place; (2) the years and months during which the sampling events took place;

238 and (3) whether the functional group/life stage under consideration was encountered or not
239 during the sampling events (0's and 1's). Encounters/non-encounters for life stages of HTL
240 groups were obtained using the body size estimates collected during surveys and body
241 length benchmarks (e.g., body length at sexual maturity) from FishBase and SeaLifeBase
242 (Froese and Pauly, 2015; Palomares and Pauly, 2015). As we extracted information for the
243 functional groups and life stages, we gauged the quality of each of the 37 survey datasets
244 (e.g., does the survey have a high or a low spatio-temporal resolution?), so as to identify
245 those survey datasets that should not be used to fit spatio-temporal binomial GLMMs for
246 the data-rich functional groups and life stages (Table 2).

247 For younger juveniles of red snapper, red grouper and gag and each of the other
248 functional groups and life stages represented in OSMOSE WFS, we determined which
249 surveys to employ when fitting spatio-temporal binomial GLMMs. To select survey data
250 from the comprehensive survey database for a given functional group/life stage and season,
251 we applied the following rules: (1) survey datasets with fewer than 50 encounters should
252 be excluded for modelling exercises (Leathwick *et al.*, 2006; Austin, 2007; Grüss *et al.*,
253 2017b); (2) years with fewer than five encounters should be excluded from modelling
254 exercises (Grüss *et al.*, 2017b); and (3) a survey dataset that we gauged to be of low quality
255 should be excluded from modelling exercises in situations that are not data-limited. Future
256 research could explore changes to criteria (1) and (2), but they are unlikely to greatly affect
257 results given that they serve to exclude surveys with little information.

258

259 ***Statistical modelling***

260 We describe our statistical modelling approach briefly here and refer the reader to
261 the Supplementary Appendix S3 for details. Our statistical modelling framework was
262 based on the spatio-temporal delta GLMM approach of Thorson *et al.* (2015), which can be

263 implemented using the R package *SpatialDeltaGLMM* (<https://github.com/nwfsc->
 264 [assess/geostatistical_delta-GLMM](https://github.com/nwfsc-assess/geostatistical_delta-GLMM)). Our spatio-temporal binomial GLMMs predict
 265 probabilities of encounter, and spatial residuals in probability of encounter are Gaussian
 266 Markov random fields that are approximated using 1000 “knots”, for the sake of
 267 computational convenience. The location of knots is determined, for each functional
 268 group/life stage, via the application of a *k*-means algorithm to the locations of the data of
 269 the comprehensive survey database; this *k*-means algorithm distributes knots spatially
 270 taking into account the sampling intensity of the different surveys considered for a given
 271 functional group/life stage.

272 Our spatio-temporal binomial GLMMs are fitted to the comprehensive survey
 273 database, following the equation:

$$g(p_i) = \sum_{t=1}^{n_t} \beta_t Y_{i,t} + \sum_{g=1}^{n_g} \gamma_g G_{i,g} + \varepsilon_{J(i)} \quad (1)$$

274 where p_i is the probability of encounter at site $s(i)$; g represents the logit link function
 275 between p_i and each random and fixed effect provided at the right side of the equation; $\varepsilon_{J(i)}$
 276 are the random effects of the spatial residuals in probability of encounter at the nearest
 277 knot to sample i , $J(i)$, on the logit scale; $\sum_{t=1}^{n_t} \beta_t Y_{i,t}$ is the fixed effect of year on p_i on the
 278 logit scale; and $\sum_{g=1}^{n_g} \gamma_g G_{i,g}$ is the effect of gear (i.e., research survey) on p_i on the logit
 279 scale, which is treated as a random effect through the implementation of restricted
 280 maximum likelihood (REML). Regarding the fixed effect of year, $Y_{i,t}$ is a design matrix
 281 where $Y_{i,t}$ is one for the year t during which sample i was collected and zero otherwise; β_t
 282 is an intercept that varies among years; and n_t is the number of sampling years for the
 283 functional group/life stage under consideration. Regarding the random effect of gear, $G_{i,g}$
 284 is a design matrix where $G_{i,g}$ is one for the gear g used to collect sample i and zero
 285 otherwise; γ_g is a gear effect (where $\gamma_g = 0$ for the gear g with the largest sample size for

286 a given functional group/life stage; this constraint is imposed for identifiability of all year
 287 effects β_t); and n_g is the number of sampling gears for the functional group/life stage
 288 under consideration. Finally, the random effects of the spatial residuals in probability of
 289 encounter are Gaussian Markov random fields that follow a multivariate normal
 290 distribution:

$$\boldsymbol{\varepsilon} \sim MN(\boldsymbol{\mu}, \boldsymbol{\Sigma}) \quad (2)$$

291 where MN is the multivariate normal distribution; $\boldsymbol{\mu}$ is the expected value at each site,
 292 which we fixed to zero; and $\boldsymbol{\Sigma}$ is a covariance matrix for $\boldsymbol{\varepsilon}$ at each site. The covariance
 293 between sites s and s' is assumed to be stationary and to follow a Matérn distribution (with
 294 smoothness $\nu = 1$):

$$\Sigma(s, s') = \sigma_\varepsilon^2 \cdot \text{Matérn}(\|\mathbf{H}(s - s')\|; \kappa) \quad (3)$$

295 where σ_ε is the standard deviation of $\boldsymbol{\varepsilon}$; \mathbf{H} is the linear transformation representing
 296 anisotropy; $(s - s') = (x - x', y - y')$ is the difference in eastings and northings between
 297 sites s and s' ; $\|\mathbf{H}(s - s')\|$ is the distance between sites after having accounted for
 298 anisotropy (Cressie and Wikle, 2015; Thorson *et al.*, 2015); and κ is the range parameter,
 299 which governs the distance over which covariance reaches 10% of its pointwise value
 300 (Thorson *et al.*, 2016). The Matérn distribution is a distribution that is commonly
 301 employed to characterize the statistical covariance between the measurements made at two
 302 distant sites (Minasny and McBratney, 2005). The Matérn covariance is stationary as used
 303 here, because it depends solely on distances between sites. It can be isotropic if distances
 304 are Euclidian distances, or follow geometric anisotropy as is the case here; geometric
 305 anisotropy is a condition where autocorrelation between locations varies with both distance
 306 and direction.

307 We estimated the fixed effect of year through maximum marginal likelihood while
 308 integrating across the random effects of gear and $\boldsymbol{\varepsilon}$; maximum marginal likelihood was

309 approximated via the Laplace approximation implemented in the Template Model Builder
310 (Kristensen *et al.*, 2016). Firstly, the probability of the random effects was approximated
311 through the use of the stochastic partial differential equation approximation (*Lindgren et*
312 *al.*, 2011) for Gaussian Markov random fields with anisotropy described in Thorson *et al.*
313 (2015). Secondly, the marginal likelihood was maximized through conventional non-linear
314 optimization in R (R Core Development Team, 2013).

315 To evaluate GLMM fits, we calculated Pearson residuals for the samples
316 considered for each functional group/life stage, as described in Supplementary Appendix
317 S3.

318

319 ***Production of distribution maps and analyses***

320 We produced probability of encounter maps for the U.S. GOM for younger
321 juveniles of red snapper, red grouper and gag and the other functional groups and life
322 stages represented in the OSMOSE-WFS ecosystem model, using the fitted spatio-
323 temporal binomial GLMMs. To produce these maps, we first defined prediction grids for
324 each of the functional groups/life stages. To do so, we constructed a spatial grid covering
325 the whole U.S. GOM (Figure 4a). Then, we generated prediction grids for each of the
326 functional groups/life stages, based on the ranges of bottom depth, latitude and longitude at
327 which the functional groups/life stages are encountered by surveys (Figures 4b-d and
328 Supplementary Figure S4). To determine the bottom depth at which the different functional
329 groups/life stages are encountered by surveys, we constructed a raster of bottom depth with
330 a resolution of 0.18° from the SRTM30 PLUS global bathymetry grid, which we obtained
331 from the Gulf of Mexico Coastal Observing System (<http://gcoos.tamu.edu/>). The way we
332 defined prediction grids for the functional groups and life stages represented in OSMOSE-
333 WFS is reasonable, because the survey data that we used to fit spatio-temporal binomial

334 GLMMs for all these functional groups/life stages - except younger juvenile gag - cover
335 the whole U.S. GOM (Supplementary Figure S5). Based on the criteria established above,
336 only three fisheries-independent surveys conducted on the West Florida Shelf (FLBAY,
337 FLHAUL, and FLTRAWL; Table 2) provided a reasonable amount of encounter/non-
338 encounter data for younger juvenile gag; the data provided by the three surveys cover the
339 eight regions of the West Florida Shelf where younger juvenile gag is consistently found
340 according to Ingram *et al.* (2013) (Supplementary Figure S5).

341 To produce the probability of encounter maps for the U.S. GOM for the different
342 functional groups/life stages, we assumed that the Gaussian Markov random field in each
343 cell of a prediction grid is equal to the value of the random field at the nearest knot. First,
344 for each of the functional groups/life stages, we constructed a probability of encounter map
345 for each sampling year, using the fitted spatio-temporal binomial GLMM for that
346 functional group/life stage. Then, we averaged the probability of encounter maps for each
347 individual sampling year to obtain one long-term probability of encounter map for each
348 functional group/life stage.

349 We used the long-term probability of encounter maps for the U.S. GOM for the
350 different functional groups/life stages to generate distribution maps for the OSMOSE-WFS
351 ecosystem model (Figure 2a). Since the prediction grids and the OSMOSE-WFS model
352 have the same spatial resolution (0.18°), we did not need to average the probabilities of
353 encounter predicted for the whole U.S. GOM according to OSMOSE-WFS grid cells.
354 However, we rescaled probabilities so that their sum across OSMOSE-WFS grid cells is
355 1.0 (hereafter referred to as “probabilities of presence”); we needed to do this so that our
356 distribution maps are useable in OSMOSE.

357 Below, we report the production and evaluation of distribution maps for the
358 functional groups and life stages represented in OSMOSE-WFS, with a focus on younger

359 juveniles of red snapper, red grouper and gag. Moreover, we estimate the mean bottom
360 depth at which younger juveniles of red snapper, red grouper and gag are encountered from
361 their long-term probability of encounter maps for the U.S. GOM and the map of bottom
362 depth (weighted average). Finally, we estimate the percentages of spatial overlap between
363 younger juveniles of red snapper, red grouper and gag and the older juvenile and adult
364 stages of red grouper and gag in the region covered by the OSMOSE-WFS model. The
365 percentage of spatial overlap between younger juvenile stage i and older juvenile or adult
366 stage j ($SO_{i,j}$) is evaluated as (Drapeau *et al.*, 2004; Brodeur *et al.*, 2008):

$$SO_{i,j} = \frac{N_{i,j}}{N_i} \cdot 100 \quad (4)$$

367 where $N_{i,j}$ is the number of cells of the OSMOSE-WFS model that are hotspots of both
368 stages i and j ; and N_i is the number of cells of the OSMOSE-WFS model that are hotspots
369 of stage i ; here, the hotspots of a given stage s are the cells of the OSMOSE-WFS model
370 where the probability of presence of stage s is equal to or greater than the mean probability
371 of presence of stage s over the entire spatial domain of OSMOSE-WFS (Brodeur *et al.*,
372 2008, 2014). The SO metric describes how older and adult grouper stages are distributed
373 spatially in relation to younger juveniles of red snapper, red grouper and gag; it serves as a
374 proxy of the exposure of younger juvenile fish to older juvenile and adult grouper stages,
375 which represent potential predators of younger juvenile fish in OSMOSE-WFS (Grüss *et al.*
376 *et al.*, 2016b, 2016c). We evaluate the SO metric to revisit a contentious result obtained with
377 the latest published versions of OSMOSE-WFS; the latest versions of OSMOSE-WFS
378 predicted younger juvenile red snapper to be preyed upon by older juveniles and adults of
379 red grouper and gag, which is something that is not reported in the literature (Grüss *et al.*,
380 2016b, 2016c).

381

382 **Results**

383 ***Compilation of a comprehensive survey database for the GOM***

384 The datasets and sampling years included in the comprehensive survey database for
385 the GOM varied greatly from one functional group/life stage to another (Supplementary
386 Table S2). We were able to follow the criteria established in the Material and methods for
387 all functional groups and life stages, except younger juvenile red grouper. In the case of
388 younger juvenile red grouper, encounters were so scarce that we retained two research
389 survey datasets with fewer than 50 encounters (Table 3). We were able to compile data to
390 generate nearly all the distribution maps that should ideally be produced according to our
391 literature review reported in Supplementary Table S2 (e.g., three maps for red grouper,
392 since the species undertake two ontogenetic migrations during its life cycle, one at age 1
393 and the other at age 3; Saul *et al.*, 2012; Carruthers *et al.*, 2015). However, due to data
394 availability, we were unable to compile data to generate seasonal distribution maps for
395 juveniles and adults of king mackerel (*Scomberomorus cavalla*) or annual maps for
396 juveniles and adults of reef omnivores. Moreover, since the OSMOSE-WFS ecosystem
397 model is not sex-structured, we did not compile data for males and females of adult gag
398 and large crabs, but rather for the entire populations of adult gag and large crabs. Finally,
399 due to a dearth of data for meiofauna and small infauna, we were unable to compile data to
400 generate distribution maps for these two LTL benthic functional groups. The only research
401 survey that encountered meiofauna and small infauna was the DGOMB fisheries-
402 independent survey, which has a low spatio-temporal resolution and was therefore gauged
403 to be of low quality for the purpose of this study (Table 2). Following Okey and
404 Mahmoudi (2002), we assumed that the spatial distributions of meiofauna and small
405 infauna are identical to that of small mobile epifauna (Supplementary Table S2).

406 Younger juvenile red snapper was encountered both in the eastern GOM (i.e., on
407 the West Florida Shelf) and in the western GOM (Table 3). For younger juvenile red

408 snapper, one observer program (OBSSHRIMP: 12,270 encounters) and three fisheries-
409 independent surveys (SMALLPEL: 166 encounters; TRAWL: 4,144; TXTRAWL: 1,480)
410 were retained for the comprehensive survey database. In these four datasets, the percentage
411 of younger juvenile red snappers encountered in the eastern GOM varied between 0
412 (TXTRAWL) and 7.9% (OBSSHRIMP).

413 In the case of younger juvenile red grouper, a total of three fisheries-independent
414 survey datasets were retained for the comprehensive survey database: FLTRAWL (59
415 encounters), TRAWL (44), and FLHAUL (29) (Table 3). The three surveys encountered
416 younger juvenile red grouper on the West Florida Shelf only.

417 Younger juvenile gag was more frequently encountered than younger juvenile red
418 grouper (Table 3). For younger juvenile gag, three fisheries-independent surveys
419 conducted in West Florida waters were retained for the comprehensive survey database:
420 FLHAUL (532 encounters), FLTRAWL (348), and FLBAY (87).

421

422 *Statistical modelling*

423 For all the functional groups/life stages, we found that none of the parameters H , κ
424 and σ_e hit an upper or lower bound, that the absolute value of the final gradient for each of
425 these parameters was smaller than 0.002, and that the Hessian matrix was positive definite
426 (Supplementary Table S6). Thus, there was no evidence of non-convergence for any of the
427 functional groups and life stages.

428 For all the functional groups and life stages, observed encounter frequencies for
429 either low or high probability samples were usually within or extremely close to the 95%
430 confidence interval for predicted probability of encounter (Supplementary Figure S7).
431 However, in the cases of older juvenile red snapper and the sardine-herring-scad complex
432 in spring-summer, observed encounter frequency for the highest probability samples

433 tended to be noticeably smaller than the 95% confidence interval for predicted probability
434 of encounter (Supplementary Figure S7). Yet, the GLMMs for these two groups did not
435 systematically over- or underestimate probability of encounter in any area of the U.S.
436 GOM (Supplementary Figure S8).

437

438 *Distribution maps*

439 The spatio-temporal binomial GLMM of younger juvenile red snapper predicted the
440 life stage to be encountered all over the GOM, primarily at bottom depths ranging from 20
441 to 60 m (43 m on average; Figure 5a). We found the probability of encounter of younger
442 juvenile red snapper to be much higher in the western than in the eastern GOM. In the
443 eastern GOM, the probability of encounter of the life stage is highest near the Florida Keys
444 and Dry Tortugas. In the western GOM, hotspots of probability of encounter for the life
445 stage include the mid-shelf zone offshore Alabama and the Texas continental shelf.

446 Younger juvenile red grouper is encountered from Apalachicola, Florida, to the
447 southern West Florida Shelf, at 24 m water depth on average (Figure 5b). Its probability of
448 encounter is highest in the southern part of the Apalachee Bay, as well as from Sarasota,
449 Florida, to the southern West Florida Shelf, in waters shallower than 40 m.

450 The spatio-temporal binomial GLMM of younger juvenile gag predicted the life
451 stage to be encountered in all of the eight regions of the West Florida Shelf where the life
452 stage has been consistently found over the recent years (Ingram *et al.*, 2013) (Figure 6).
453 We found that younger juvenile gag is encountered at a bottom depth of 8 m on average.
454 The probability of encounter of the life stage is highest in Tampa Bay (Figure 6b). It is also
455 relatively high in St. Andrew Bay and Sarasota Bay, while it is lowest in St. Joe Bay and
456 Cedar Key.

457 The distribution maps that we produced from GLMM predictions for the functional
458 groups and life stages represented in OSMOSE-WFS - including younger juveniles of red
459 snapper, red grouper and gag – are shown in Figure 7. These distribution maps allowed us
460 to evaluate percentages of spatial overlap (*SO*'s) between younger juveniles of red snapper,
461 red grouper and gag and the older juvenile and adult stages of red grouper and gag (Table
462 4). We found that younger juvenile red grouper is the stage most exposed to older juvenile
463 red grouper (*SO* = 78%), followed by younger juvenile gag (42%) and younger juvenile
464 red snapper (36%). The spatial distribution of adult red grouper strongly overlaps with
465 those of younger juvenile red grouper (*SO* = 81%) and younger juvenile red snapper (*SO* =
466 70%). Younger juvenile gag is the stage most exposed to older juvenile gag (*SO* = 72%),
467 followed by younger juvenile red snapper (21%) and younger juvenile red grouper (19%).
468 Finally, younger juvenile red snapper is the stage most exposed to adult gag (*SO* = 26%),
469 followed by younger juvenile gag (14%) and younger juvenile red grouper (8%).

470

471 **Discussion**

472 In this study, we applied the framework proposed in Grüss *et al.* (2016a) to
473 construct a database blending all of the encounter/non-encounter data of the GOM
474 collected by the fisheries-independent surveys and fisheries-dependent observer programs
475 using random sampling schemes (i.e., a “comprehensive survey database” for the GOM),
476 and to produce distribution maps for younger juveniles of red snapper, red grouper and gag
477 and the other functional groups and life stages represented in the OSMOSE-WFS
478 ecosystem model. The spatio-temporal binomial GLMMs that we fit in the present study
479 allowed us to generate maps for nearly all the functional groups and life stages represented
480 in OSMOSE-WFS, except four LTL functional groups (phytoplankton, zooplankton,
481 meiofauna, and small infauna). The probabilities of encounter predicted by all spatio-

482 temporal binomial GLMMs were demonstrated to be reasonable (Supplementary Figures
483 S7 and S8). In particular, model fits for adult gag were greatly improved in this study
484 compared to a previous study applying Grüss *et al.* (2016a)'s framework (Grüss *et al.*,
485 2017b); in Grüss *et al.* (2017b), adult gag observed frequency of encounter for the highest
486 probability samples was considerably smaller than the 95% confidence interval for
487 predicted probability of encounter, which was not the case in the present study. This result
488 stems from the consideration of additional survey datasets in the present study.

489 The compilation of a comprehensive survey database for the GOM allowed us to fit
490 spatio-temporal binomial GLMMs to then produce distribution maps for younger juveniles
491 of red snapper, red grouper and gag for the CMS biophysical model, as well as distribution
492 maps for almost all the functional groups and life stages represented in the OSMOSE-WFS
493 ecosystem model. Without the comprehensive survey database, it would have been
494 impossible to generate distribution maps for some of these functional groups and life
495 stages, particularly the younger juveniles of red grouper and gag. The functional groups for
496 which we were unable to produce distribution maps using the comprehensive survey
497 database included two LTL benthic functional groups, meiofauna and small infauna, which
498 were both encountered only by the DGOMB survey in the GOM; DGOMB is a fisheries-
499 independent survey that collected data at a limited number of sites during the summer
500 months of the period 2000-2002 in the offshore areas of the GOM only (Rowe and
501 Kennicutt, 2009). Here, we assumed that the spatial distributions of meiofauna and small
502 infauna are identical to that of small mobile epifauna, based on Okey and Mahmoudi
503 (2002). In the previous versions of the OSMOSE-WFS model (Grüss *et al.*, 2015, 2016b,
504 2016c), since we had no data for meiofauna, small infauna and small mobile epifauna, we
505 assumed a uniform spatial distribution for the three LTL functional groups. We
506 recommend the initiation of new research surveys targeting small benthic organisms in

507 both the inshore and offshore areas of the GOM, so as to collect encounter/non-encounter
508 data for meiofauna, small infauna and similar animals and fill in current gaps in the
509 comprehensive survey database. More generally, the comprehensive survey database
510 should be viewed as a dynamic platform, which should be regularly updated as new data
511 are collected by the research surveys of the GOM that use random sampling schemes
512 (Grüss *et al.*, 2016a). The functional groups for which we were unable to produce
513 distribution maps using the comprehensive survey database also included phytoplankton
514 and zooplankton. For those, no research survey data can be employed to fit statistical
515 models and then generate distribution maps. To generate monthly distribution maps for
516 phytoplankton and zooplankton, we used, respectively, SeaWiFS (Sea-viewing Wide
517 Field-of-view Sensor) chlorophyll a concentration data
518 (<http://oceancolor.gsfc.nasa.gov/SeaWiFS/>) and zooplankton biomass estimates from the
519 SEAPODYM ocean model (Lehodey *et al.*, 2010) (Supplementary Appendix S9).

520 The spatio-temporal binomial GLMMs that we fitted for the functional groups and
521 life stages represented in OSMOSE-WFS yielded reasonable predictions (Supplementary
522 Figures S7 and S8). Yet, we found that observed encounter frequency for the highest
523 probability samples tended to be noticeably smaller than the 95% confidence interval for
524 predicted encounter probability in the cases of older juvenile red snapper and the sardine-
525 herring-scad complex in spring-summer (Supplementary Figure S7). We did not integrate
526 environmental covariates in spatio-temporal binomial GLMMs in the present study,
527 because previous unpublished and published work (e.g., Drexler and Ainsworth, 2013;
528 Farmer and Karnauskas, 2013; Grüss *et al.*, 2014a) suggests that non-geospatial statistical
529 models that integrate environmental covariates result in substantial, unmodelled spatial
530 patterns in residuals for fish and invertebrates of the GOM. However, we suspect that
531 integrating environmental covariates in the spatio-temporal binomial GLMM of some

532 functional groups/life stages (e.g., natural and artificial physical habitats and vertical relief
533 in the case of older juvenile red snapper; Szedlmayer and Lee, 2004; Wells, 2007;
534 Gallaway *et al.*, 2009) may improve model fits. Therefore, we recommend future studies to
535 explore this issue.

536 The results obtained for younger juveniles of red snapper, red grouper and gag in
537 this study concur with the literature, provide additional insights into the spatial distribution
538 patterns of these life stages, and highlight important future research avenues (Box 1).
539 Importantly, producing distribution maps for younger juveniles of red snapper, red grouper
540 and gag, as well as for the older juvenile and adult stages of the three species, allowed us to
541 revisit a contentious result obtained with the latest published versions of the OSMOSE-
542 WFS model (Grüss *et al.*, 2016b, 2016c). As explained earlier, in OSMOSE, diet
543 compositions are not determined *a priori*, but rather emerges from model simulations, and
544 predation is controlled by spatial distributions, predator/prey size ratios and the
545 accessibility of prey to predators (Grüss *et al.*, 2016b; Fu *et al.*, 2017). In Grüss *et al.*
546 (2016b, 2016c), due to the predator/prey size ratios (estimated from the literature),
547 accessibility coefficients (determined from expert opinion) and distribution maps
548 (constructed in Grüss *et al.* (2014b)) fed into OSMOSE-WFS, older juveniles and adults of
549 red grouper and gag were predicted to prey upon younger juvenile red snapper. Such
550 predation events are, however, not reported in the empirical literature. Because the
551 distribution maps generated in Grüss *et al.* (2014b) are uncertain for a number of reasons
552 listed in the Introduction, the predictions made in Grüss *et al.* (2016b, 2016c) that younger
553 juvenile red snapper is preyed upon by older juveniles of adults of red grouper and gag
554 were surprising. The robust GLMMs fitted to the comprehensive survey database for the
555 GOM in this study predict that: (1) the spatial distributions of younger juvenile red snapper
556 and adult red grouper strongly overlap; (2) younger juvenile red snapper is more exposed

557 to adult gag than younger juveniles of red grouper and gag, which are both prey items of
558 adult gag according to the literature (Grüss *et al.*, 2016b, 2016c); and (3) the percentages of
559 spatial overlap between younger juvenile red snapper and older juveniles of red grouper
560 and gag are relatively small but non-negligible. Therefore, the present study shows that it is
561 reasonable to hypothesize that older juveniles and adults of red grouper and gag prey upon
562 younger juveniles of red snapper. To investigate this hypothesis further, future diet surveys
563 should collect additional stomachs for older juveniles and adults of red grouper and gag.
564 Such surveys should ideally be conducted using spearfishing rather than the gears
565 classically used to sample groupers in the GOM (e.g., longline), which result in stomachs
566 being everted when fish ascend from the depths. Moreover, because the fish ingested by
567 groupers are often unidentifiable, even to the family level, advanced DNA
568 (deoxyribonucleic acid) barcoding techniques should be used to identify precisely the
569 different fish prey of older juveniles and adults of red grouper and gag (Dahl *et al.*, 2017).

570 The framework employed in the present study is valuable for producing distribution
571 maps and functional relationships for different types of spatially-explicit ecosystem models
572 (Grüss *et al.*, 2016a), as well as for parameterizing biophysical models used to inform
573 EBFM. The spatio-temporal binomial GLMM approach used in this study can be
574 employed to generate distribution maps for any spatially-explicit ecosystem model whose
575 entire spatial domain is sampled by the research surveys included in the comprehensive
576 survey database (Grüss *et al.*, 2016a). Geospatial statistical models cannot be used to
577 construct accurate distribution maps for spatially-explicit ecosystem models whose entire
578 spatial domain is not sampled by the surveys included in the comprehensive survey
579 database (e.g., spatially-explicit ecosystem models for the entire GOM Large Marine
580 Ecosystem); for such spatially-explicit ecosystem models, it is necessary to extrapolate the
581 spatial distributions of marine organisms to unsampled areas. Binomial GAMs

582 characterized by a few covariates and smooth relationships between environmental
583 parameters and functional groups/life stages are appropriate for such spatially-explicit
584 ecosystem models (Drexler and Ainsworth, 2013; Mannocci *et al.*, 2017). The widely-used
585 Ecospace modelling platform does not employ distribution maps to allocate the biomasses
586 of modelled functional groups/life stages over space, but rather a “habitat capacity model”,
587 which defines the spatial distribution of species dynamically based on relationships
588 between abiotic environmental variables and functional groups/life stages (Christensen *et*
589 *al.*, 2014). The habitat capacity model of Ecospace applications of the GOM can be
590 parameterized using functional relationships established by fitting binomial GAMs to the
591 comprehensive survey database (Grüss *et al.*, 2016a). The framework applied in this study
592 is also useful to parameterize biophysical models designed to predict annual recruitment
593 anomalies due to oceanographic factors for assessed species, such as the CMS (Karnauskas
594 *et al.*, 2013a, 2013b; Grüss *et al.*, 2014b). In the present study, we focused on the
595 production of distribution maps for younger juvenile fish for defining larval settlement
596 areas in biophysical models. The framework applied in this study can also be employed to
597 generate maps of egg production from distribution maps for adult life stages, under the
598 assumption that egg production is proportional to the probability of encounter of adult fish
599 (Grüss *et al.*, 2014b).

600

601 **Supplementary data**

602 Supplementary material is available at the *ICESJMS* online version of the manuscript.

603

604 **Acknowledgments**

605 This work was funded in part by the Florida RESTORE Act Centers of Excellence
606 Research Grants Program, Subagreement No. 2015-01-UM-522, and the National Oceanic

607 and Atmospheric Administration's RESTORE Act Science Program under award
608 NA15NOS4510233 to the University of Miami. This manuscript has cleared an internal
609 review at the NOAA Northwest Fisheries Science Center. We are grateful to Isaac Kaplan,
610 the NOAA internal reviewer, as well as to the Editor and two anonymous reviewers, whose
611 comments have improved the quality of the present manuscript. We would like to thank
612 Walt Ingram for having provided us with shapefiles for the eight regions of the West
613 Florida Shelf where younger juvenile gag has been consistently found over the recent
614 years. We are grateful to the following people for having provided us with data for the
615 comprehensive survey database for the Gulf of Mexico: Adam G. Pollack, Alisha Gray,
616 April Cook, Beverly Sauls, Brandi Noble, Chris Gardner, Christy Pattengill-Semmens,
617 Doug DeVries, Elizabeth Scott-Denton, Evan John Anderson, Fernando Martinez-Andrade,
618 Gilbert Rowe, Jeff Rester, Jill Hendon, John Carlson, John Mareska, Kelly Fitzpatrick,
619 Kenneth Brennan, Lawrence Beerkircher, Matthew A. Nuttall, Matthew D. Campbell,
620 Mike Brainard, Mike Harden, Nicole Smith, Rick Burris, Steve Turner, Theodore S.
621 Switzer, Tim MacDonald, and Tracey T. Sutton. The PCTRAP, PCVIDEO, GULFSPAN,
622 OBSLL, OBSVL, OBSSHRIMP, OBSGILL, SBLOP and POP data products were
623 produced without the involvement of NOAA Fisheries staff, and NOAA Fisheries cannot
624 vouch for the validity of these products. The TRAWL and INBLL data were produced
625 without the involvement of SEAMAP partners. Therefore, SEAMAP and its partners
626 cannot vouch for the validity of these products. The FLBAY, FLHAUL, FLOBS,
627 FLPURSE, FLTRAP, FLTRAWL and FLVIDEO data products were produced without the
628 involvement of FWC – FWRI staff, and FWC – FWRI cannot vouch for the validity of
629 these products. The ALGILL data products were produced without the involvement of
630 AMRD staff, and AMRD cannot vouch for the validity of these products; a portion of the
631 provided data was funded through a Fish and Wildlife Service Sport Fish Restoration

632 Program grant. The MSGILL and MSHAND data products were produced without the
633 involvement of USM GCRL staff, and USM GCRL staff cannot vouch for the validity of
634 these products; the collection of MSGILL data was funded through a collaboration with the
635 Mississippi Department of Marine Resources by a U.S. Fish and Wildlife Service Sport
636 Fish Restoration Program grant. The LAVL data products were produced without the
637 involvement of LDWF staff and, therefore, LDWF cannot vouch for the validity of these
638 products. Many thanks to Patrick Lehodey, Beatriz Calmettes, Chris Koenig, Gary
639 Fitzhugh, Matt Love, Michael Drexler, Skyler R. Sagarese, John F. Walter III, Mary
640 Christman, and David Gloeckner for having provided help or advice at different levels of
641 this study.

642

643 **References**

- 644 Austin, M. 2007. Species distribution models and ecological theory: a critical assessment
645 and some possible new approaches. *Ecological Modelling*, 200: 1–19.
- 646 Brodeur, R. D., Suchman, C. L., Reese, D. C., Miller, T. W., and Daly, E. A. 2008. Spatial
647 overlap and trophic interactions between pelagic fish and large jellyfish in the
648 northern California Current. *Marine Biology*, 154: 649–659.
- 649 Brodeur, R. D., Barceló, C., Robinson, K. L., Daly, E. A., and Ruzicka, J. J. 2014. Spatial
650 overlap between forage fishes and the large medusa *Chrysaora fuscescens* in the
651 northern California Current region. *Marine Ecology Progress Series*, 510: 167–181.
- 652 Bullock, L. H., and Smith, G. B. 1991. Seabasses (Pisces: Serranidae). *Memoirs of the*
653 *Hourglass Cruises VIII (II) Florida Marine Research Institute. Department of*
654 *Natural Resources, St. Petersburg, Florida, USA.*
- 655 Carruthers, T. R., Walter, J. F., McAllister, M. K., Bryan, M. D., and Wilberg, M. 2015.
656 Modelling age-dependent movement: an application to red and gag groupers in the
657 Gulf of Mexico. *Canadian Journal of Fisheries and Aquatic Sciences*, 72: 1159–
658 1176.
- 659 Casey, J. P., Poulakis, G. R., and Stevens, P. W. 2007. Habitat use by juvenile gag,
660 *Mycteroperca microlepis* (Pisces: Serranidae), in subtropical Charlotte Harbor,
661 Florida (USA). *Gulf and Caribbean Research*, 19: 1–9.
- 662 Chagaris, D. D. 2013. Ecosystem-based evaluation of fishery policies and tradeoffs on the
663 West Florida Shelf. PhD thesis, University of Florida, Gainesville, Florida.
- 664 Christensen, V., Coll, M., Steenbeek, J., Buszowski, J., Chagaris, D., and Walters, C. J.
665 2014. Representing variable habitat quality in a spatial food web model.
666 *Ecosystems*, 17: 1397–1412.
- 667 Coleman, F. C., Koenig, C. C., Scanlon, K. M., Heppell, S., Heppell, S., and Miller, M. W.
668 2010. Benthic habitat modification through excavation by red grouper, *Epinephelus*
669 *morio*, in the northeastern Gulf of Mexico. *The Open Fish Science Journal*, 3.

- 670 Coleman, F. C., Scanlon, K. M., and Koenig, C. C. 2011. Groupers on the edge: shelf edge
671 spawning habitat in and around marine reserves of the northeastern Gulf of Mexico.
672 *The Professional Geographer*, 63: 456–474.
- 673 Cressie, N., Wikle, C.K., 2015. *Statistics for spatio-temporal data*. John Wiley & Sons,
674 Hoboken, NJ.
- 675 Dahl, K. A., Patterson, W. F., Robertson, A., and Ortmann, A. C. 2017. DNA barcoding
676 significantly improves resolution of invasive lionfish diet in the Northern Gulf of
677 Mexico. *Biological Invasions*, doi: 10.1007/s10530-017-1407-3.
- 678 Drapeau, L., Pecquerie, L., Fréon, P., and Shannon, L. J. 2004. Quantification and
679 representation of potential spatial interactions in the southern Benguela ecosystem.
680 *African Journal of Marine Science*, 26: 141–159.
- 681 Drexler, M., and Ainsworth, C. H. 2013. Generalized additive models used to predict
682 species abundance in the Gulf of Mexico: an ecosystem modeling tool. *PLoS ONE*,
683 8: e64458.
- 684 Farmer, N. A., and Karnauskas, M. 2013. Spatial distribution and conservation of speckled
685 hind and warsaw grouper in the Atlantic Ocean off the southeastern US. *PloS One.*,
686 8: e78682.
- 687 Fitzhugh, G. R., Koenig, C. C., Coleman, F. C., Grimes, C. B., and Sturges, W. 2005.
688 Spatial and temporal patterns in fertilization and settlement of young gag
689 (*Mycteroperca microlepis*) along the West Florida Shelf. *Bulletin of Marine
690 Science*, 77: 377–396.
- 691 Froese, R., and Pauly, D. 2015. A Global Information System on Fishes, Fishbase,
692 <http://www.fishbase.org>.
- 693 Fu, C., Olsen, N., Taylor, N., Grüss, A., Batten, S., Liu, H., Verley, P., *et al.* 2017. Spatial
694 and temporal dynamics of predator-prey species interactions off western Canada.
695 *ICES Journal of Marine Science*, doi: 10.1093/icesjms/fsx056.
- 696 Fulton, E. A., Parslow, J. S., Smith, A. D., and Johnson, C. R. 2004. Biogeochemical
697 marine ecosystem models II: the effect of physiological detail on model
698 performance. *Ecological Modelling*, 173: 371–406.
- 699 Fulton, E. A., Link, J. S., Kaplan, I. C., Savina-Rolland, M., Johnson, P., Ainsworth, C.,
700 Horne, P., *et al.* 2011. Lessons in modelling and management of marine
701 ecosystems: the Atlantis experience. *Fish and Fisheries*, 12: 171–188.
- 702 Gallaway, B. J., Cole, J. G., Meyer, R., and Roscigno, P. 1999. Delineation of essential
703 habitat for juvenile red snapper in the northwestern Gulf of Mexico. *Transactions
704 of the American Fisheries Society*, 128: 713–726.
- 705 Gallaway, B. J., Szedlmayer, S. T., and Gazey, W. J. 2009. A life history review for red
706 snapper in the Gulf of Mexico with an evaluation of the importance of offshore
707 petroleum platforms and other artificial reefs. *Reviews in Fisheries Science*, 17:
708 48–67.
- 709 Grüss, A., Karnauskas, M., Sagarese, S. R., Paris, C. B., Zapfe, G., Walter III, J. F.,
710 Ingram, W., *et al.* 2014a. Use of the Connectivity Modeling System to estimate the
711 larval dispersal, settlement patterns and annual recruitment anomalies due to
712 oceanographic factors of red grouper (*Epinephelus morio*) on the West Florida
713 Shelf. SEDAR42-DW-03, SEDAR, North Charleston, SC. 24 pp.
- 714 Grüss, A., Drexler, M., and Ainsworth, C. H. 2014b. Using delta generalized additive
715 models to produce distribution maps for spatially explicit ecosystem models.
716 *Fisheries Research*, 159: 11–24.
- 717 Grüss, A., Schirripa, M. J., Chagaris, D., Drexler, M., Simons, J., Verley, P., Shin, Y.-J., *et
718 al.* 2015. Evaluation of the trophic structure of the West Florida Shelf in the 2000s
719 using the ecosystem model OSMOSE. *Journal of Marine Systems*, 144: 30–47.

- 720 Grüss, A., Babcock, E. A., Sagarese, S. R., Drexler, M., Chagaris, D. D., Ainsworth, C. H.,
721 Penta, B., *et al.* 2016a. Improving the spatial allocation of functional group
722 biomasses in spatially-explicit ecosystem models: insights from three Gulf of
723 Mexico models. *Bulletin of Marine Science*, 92: 473–496.
- 724 Grüss, A., Schirripa, M. J., Chagaris, D., Velez, L., Shin, Y.-J., Verley, P., Oliveros-
725 Ramos, R., *et al.* 2016b. Estimating natural mortality rates and simulating fishing
726 scenarios for Gulf of Mexico red grouper (*Epinephelus morio*) using the ecosystem
727 model OSMOSE-WFS. *Journal of Marine Systems*, 154: 264–279.
- 728 Grüss, A., Harford, W. J., Schirripa, M. J., Velez, L., Sagarese, S. R., Shin, Y.-J., and
729 Verley, P. 2016c. Management strategy evaluation using the individual-based,
730 multispecies modeling approach OSMOSE. *Ecological Modelling*, 340: 86–105.
- 731 Grüss, A., Rose, K. A., Simons, J., Ainsworth, C. H., Babcock, E. A., Chagaris, D. D., De
732 Mutsert, K., *et al.* 2017a. Recommendations on the use of ecosystem modeling for
733 informing ecosystem-based fisheries management and restoration outcomes in the
734 Gulf of Mexico. *Marine and Coastal Fisheries*, doi:
735 10.1080/19425120.2017.1330786.
- 736 Grüss, A., Thorson, J. T., Sagarese, S. R., Babcock, E. A., Karnauskas, M., Walter, J. F.,
737 and Drexler, M. 2017b. Ontogenetic spatial distributions of red grouper
738 (*Epinephelus morio*) and gag grouper (*Mycteroperca microlepis*) in the US Gulf of
739 Mexico. *Fisheries Research*, 193: 129–142.
- 740 Halouani, G., Lasram, F. B. R., Shin, Y.-J., Velez, L., Verley, P., Hattab, T., Oliveros-
741 Ramos, R., *et al.* 2016. Modelling food web structure using an end-to-end approach
742 in the coastal ecosystem of the Gulf of Gabes (Tunisia). *Ecological Modelling*, 339:
743 45–57.
- 744 Harvey, C. J., Kelble, C. R., and Schwing, F. B. 2017. Implementing “the IEA”: using
745 integrated ecosystem assessment frameworks, programs, and applications in
746 support of operationalizing ecosystem-based management. *ICES Journal of Marine
747 Science*, 74: 398–405.
- 748 Hastings, R. W. 1979. The origin and seasonality of the fish fauna on a new jetty in the
749 northeastern Gulf of Mexico. *Bulletin of the Florida State Museum, Biological
750 Science*, 24: 1–22.
- 751 Ingram, G. W., Pollack, A., and McEachron, L. 2013. Summary of fishery-independent
752 surveys of juvenile gag grouper in the Gulf of Mexico. SEDAR33-AW06. SEDAR,
753 North Charleston, SC. 20 pp.
- 754 Johnson, D. R., Perry, H. M., and Lyczkowski-Shultz, J. 2013. Connections between
755 Campeche Bank and red snapper populations in the Gulf of Mexico via modeled
756 larval transport. *Transactions of the American Fisheries Society*, 142: 50–58.
- 757 Karnauskas, M., Walter, J. F., and Paris, C. B. 2013a. Use of the Connectivity Modeling
758 System to estimate movements of red snapper (*Lutjanus campechanus*) recruits in
759 the northern Gulf of Mexico. SEDAR31-AW10. SEDAR, North Charleston, SC, 20
760 pp.
- 761 Karnauskas, M., Zapfe, G., Grüss, A., Walter III, J. F., and Schirripa, M. J. 2013b. Use of
762 the Connectivity Modeling System to estimate movements of gag grouper
763 (*Mycteroperca microlepis*) recruits in the northern Gulf of Mexico. SEDAR33-
764 DW18. SEDAR, North Charleston, SC 12 pp.
- 765 Koenig, C. C., and Coleman, F. C. 1998. Absolute abundance and survival of juvenile gags
766 in sea grass beds of the northeastern Gulf of Mexico. *Transactions of the American
767 Fisheries Society*, 127: 44–55.
- 768 Koenig, C. C., and Coleman, F. C. 1999. Recruitment indices and seagrass habitat
769 relationships of the early juvenile stages of gag, gray snapper, and other

770 economically important reef fishes in the eastern Gulf of Mexico. Final Report,
771 MARFIN Award No. NA57FF0055.

772 Kristensen, K., Nielsen, A., Berg, C. W., Skaug, H., and Bell, B. 2016. TMB: automatic
773 differentiation and Laplace approximation. *Journal of Statistical Software*, 70: 1–
774 21.

775 Leathwick, J. R., Elith, J., and Hastie, T. 2006. Comparative performance of generalized
776 additive models and multivariate adaptive regression splines for statistical
777 modelling of species distributions. *Ecological Modelling*, 199: 188–196.

778 Lehodey, P., Murtugudde, R., and Senina, I. 2010. Bridging the gap from ocean models to
779 population dynamics of large marine predators: a model of mid-trophic functional
780 groups. *Progress in Oceanography*, 84: 69–84.

781 Levin, P. S., Kelble, C. R., Shuford, R. L., Ainsworth, C., Dunsmore, R., Fogarty, M. J.,
782 Holsman, K., *et al.* 2014. Guidance for implementation of integrated ecosystem
783 assessments: a US perspective. *ICES Journal of Marine Science*, 71: 1198–1204.

784 Lindgren, F., Rue, H. avard, and Lindström, J. 2011. An explicit link between Gaussian
785 fields and Gaussian Markov random fields: the stochastic partial differential
786 equation approach. *Journal of the Royal Statistical Society: Series B (Statistical
787 Methodology)*, 73: 423–498.

788 Mace, P. M., Bartoo, N. W., Hollowed, A. B., Kleiber, P., Methot, R. D., Murawski, S. A.,
789 Powers, J. E., *et al.* 2001. Marine fisheries stock assessment improvement plan.
790 Report of the National Marine Fisheries Service. National Task Force for
791 Improving Fish Stock Assessments, US Department of Commerce and NOAA, 68
792 pp.

793 Mannocci, L., Roberts, J.J., Miller, D.L., Halpin, P.N., 2017. Extrapolating cetacean
794 densities to quantitatively assess human impacts on populations in the high seas.
795 *Conservation Biology*, 31: 601-614.

796 Minasny, B., and McBratney, A. B. 2005. The Matérn function as a general model for soil
797 variograms. *Geoderma*, 128: 192–207.

798 Moe, M. A. 1969. Biology of the red grouper *Epinephelus morio* (Valenciennes) from the
799 eastern Gulf of Mexico. Florida Department of Natural Resources Marine Research
800 Laboratory Professional papers series, 10: 1–95.

801 Monk, M. H., Powers, J. E., and Brooks, E. N. 2015. Spatial patterns in species
802 assemblages associated with the northwestern Gulf of Mexico shrimp trawl fishery.
803 *Marine Ecology Progress Series*, 519: 1–12.

804 MSFCMA. 2007. Magnuson-Stevens Fishery Conservation and Management Act. U.S.
805 Department of Commerce NOAA, National Marine Fisheries Service.

806 Mullaney Jr, M.D., 1994. Ontogenetic shifts in diet of gag, *Mycteroperca*
807 *microlepis*, (Goode and Bean), (Pisces: Serranidae). *Proceedings of the Gulf and*
808 *Caribbean Fisheries Institute*, 43: 432–445.

809 NOS. 2008. Gulf of Mexico at a Glance: U.S. National Ocean Service, Department of
810 Commerce, National Oceanic and Atmospheric Administration. Washington, DC.

811 Okey, T. A., and Mahmoudi, B. 2002. An Ecosystem Model of the West Florida Shelf for
812 use in Fisheries Management and Ecological Research: Volume II. Model
813 Construction. Report of the Florida Marie Research Institute, St Petersburg,
814 Florida, USA.

815 Palomares, M. L. D., and Pauly, D. 2015. SeaLifeBase. Available:
816 <http://http://www.sealifebase.org>.

817 Paris, C. B., Helgers, J., Van Sebille, E., and Srinivasan, A. 2013. Connectivity Modeling
818 System: A probabilistic modeling tool for the multi-scale tracking of biotic and
819 abiotic variability in the ocean. *Environmental Modelling & Software*, 42: 47–54.

820 R Core Development Team. 2013. R: A Language and Environment for Statistical
821 Computing. R Foundation for Statistical Computing, Vienna, Austria.
822 <http://www.R-project.org/>.

823 Rowe, G. T., and Kennicutt, M. C. 2009. Northern Gulf of Mexico continental slope
824 habitats and benthic ecology study: Final report. OCS Study MMS 2009-039. 456
825 pp.

826 Samhuri, J. F., Haupt, A. J., Levin, P. S., Link, J. S., and Shuford, R. 2014. Lessons
827 learned from developing integrated ecosystem assessments to inform marine
828 ecosystem-based management in the USA. *ICES Journal of Marine Science*, 71:
829 1205–1215.

830 Saul, S., Die, D., Brooks, E. N., and Burns, K. 2012. An individual-based model of
831 ontogenetic migration in reef fish using a biased random walk. *Transactions of the*
832 *American Fisheries Society*, 141: 1439–1452.

833 Shin, Y.-J., and Cury, P. 2001. Exploring fish community dynamics through size-
834 dependent trophic interactions using a spatialized individual-based model. *Aquatic*
835 *Living Resources*, 14: 65–80.

836 Shin, Y.-J., and Cury, P. 2004. Using an individual-based model of fish assemblages to
837 study the response of size spectra to changes in fishing. *Canadian Journal of*
838 *Fisheries and Aquatic Sciences*, 61: 414–431.

839 Switzer, T. S., MacDonald, T. C., McMichael Jr, R. H., and Keenan, S. F. 2012.
840 Recruitment of juvenile Gags in the eastern Gulf of Mexico and factors
841 contributing to observed spatial and temporal patterns of estuarine occupancy.
842 *Transactions of the American Fisheries Society*, 141: 707–719.

843 Switzer, T. S., Keenan, S. F., Stevens, P. W., McMichael Jr, R. H., and MacDonald, T. C.
844 2015. Incorporating Ecology into Survey Design: Monitoring the Recruitment of
845 Age-0 Gags in the Eastern Gulf of Mexico. *North American Journal of Fisheries*
846 *Management*, 35: 1132–1143.

847 Szedlmayer, S. T., and Conti, J. 1999. Nursery habitats, growth rates, and seasonality of
848 age-0 red snapper, *Lutjanus campechanus*, in the northeast Gulf of Mexico. *Fishery*
849 *Bulletin*, 97: 626–635.

850 Szedlmayer, S. T., and Lee, J. D. 2004. Diet shifts of juvenile red snapper (*Lutjanus*
851 *campechanus*) with changes in habitat and fish size. *Fishery Bulletin*, 102: 366–
852 375.

853 Szedlmayer, S. T., and Mudrak, P. A. 2014. Influence of age-1 conspecifics, sediment
854 type, dissolved oxygen, and the Deepwater Horizon oil spill on recruitment of age-
855 0 red snapper in the northeast Gulf of Mexico during 2010 and 2011. *North*
856 *American Journal of Fisheries Management*, 34: 443–452.

857 Thorson, J. T., Shelton, A. O., Ward, E. J., and Skaug, H. J. 2015. Geostatistical delta-
858 generalized linear mixed models improve precision for estimated abundance
859 indices for West Coast groundfishes. *ICES Journal of Marine Science*, 72: 1297–
860 1310.

861 Thorson, J. T., Fonner, R., Haltuch, M. A., Ono, K., and Winker, H. 2016. Accounting for
862 spatiotemporal variation and fisher targeting when estimating abundance from
863 multispecies fishery data 1. *Canadian Journal of Fisheries and Aquatic Sciences*,
864 73: 1–14.

865 Wells, R. J. D. 2007. The effects of trawling and habitat use on red snapper and the
866 associated community. Ph.D. thesis, Louisiana State University, Baton Rouge,
867 Louisiana.

868 Workman, I., Shah, A., Foster, D., and Hataway, B. 2002. Habitat preferences and site
869 fidelity of juvenile red snapper (*Lutjanus campechanus*). ICES Journal of Marine
870 Science, 59: S43–S50.
871 <http://gcoos.tamu.edu/>
872 https://github.com/nwfsc-assess/geostatistical_delta-GLMM
873 <http://oceancolor.gsfc.nasa.gov/SeaWiFS/>

874 **Tables**

875 **Table 1.** Functional groups represented in the OSMOSE-WFS ecosystem model, including
876 high trophic level (HTL) groups, whose entire life cycle is simulated in OSMOSE-WFS,
877 and low trophic level (LTL) groups, whose biomass is used to force the model. Species of
878 a given HTL group exhibit similar life history characteristics, body size ranges, diets and
879 exploitation patterns. Some individual species constitute their own HTL group, as they are
880 emblematic to the West Florida Shelf and of high economic importance. A reference
881 species was identified for each of the HTL groups (indicated in bold).

Functional group	HTL or LTL group?	Species making up the functional group
King mackerel	HTL	King mackerel (<i>Scomberomorus cavalla</i>)
Amberjacks	HTL	Greater amberjack (<i>Seriola dumerili</i>), banded rudderfish (<i>Seriola zonata</i>), lesser amberjack (<i>Seriola fasciata</i>), almaco jack (<i>Seriola rivoliana</i>)
Red grouper	HTL	Red grouper (<i>Epinephelus morio</i>)
Gag	HTL	Gag (<i>Mycteroperca microlepis</i>)
Red snapper	HTL	Red snapper (<i>Lutjanus campechanus</i>)
Sardine-herring-scad complex	HTL	Scaled sardine (<i>Harengula jaguana</i>), Spanish sardine (<i>Sardinella aurita</i>), Atlantic thread herring (<i>Opisthonema oglinum</i>), round scad (<i>Decapterus punctatus</i>), menhaden (<i>Brevoortia</i> spp.)
Anchovies and silversides	HTL	Bay anchovy (<i>Anchoa mitchilli</i>), striped anchovy (<i>Anchoa hepsetus</i>), silversides (Atherinidae spp.), alewife (<i>Alosa</i> spp.)
Coastal omnivores	HTL	Pinfish (<i>Lagodon rhomboides</i>), spottail pinfish (<i>Diplodus holbrooki</i>), orange filefish (<i>Aluterus schoepfii</i>), fringed filefish (<i>Monacanthus ciliatus</i>), planehead filefish (<i>Monacanthus hispidus</i>), orangespotted filefish (<i>Cantherhines pullus</i>), honeycomb filefish (<i>Acanthostracion polygonius</i>), Atlantic spadefish (<i>Chaetodipterus faber</i>), scrawled cowfish (<i>Lactophrys quadricornis</i>), pufferfish (Tetraodontidae spp.)
Reef carnivores	HTL	White grunt (<i>Haemulon plumieri</i>), black sea bass (<i>Centropristis striata</i>), rock sea bass (<i>Centropristis philadelphica</i>), belted sandfish (<i>Serranus subligarius</i>), longtail bass (<i>Hemanthias leptus</i>), butter hamlet (<i>Hypoplectus unicolor</i>), creole fish (<i>Paranthias furcifer</i>), splippery dick (<i>Halichoeres bivittatus</i>), painted wrasse (<i>Halichoeres caudalis</i>), yellowhead wrasse (<i>Halichoeres garnoti</i>), bluehead (<i>Thalassoma bifasciatum</i>), reef croaker (<i>Odontoscion dentex</i>), jackknife-fish (<i>Equetus lanceatus</i>), leopard toadfish (<i>Opsanus pardus</i>), scorpion fish (Scorpaenidae spp.), bigeyes (Priacanthidae spp.), littlehead porgy (<i>Calamus proridens</i>), jolthead porgy (<i>Calamus bajonado</i>), saucereye progy (<i>Calamus calamus</i>), whitebone progy (<i>Calamus leucosteus</i>), knobbed progy (<i>Calamus nodosus</i>), French grunt (<i>Haemulon flavolineatum</i>), Spanish grunt (<i>Haemulon macrostomum</i>), margate (<i>Haemulon album</i>), bluestriped grunt (<i>Haemulon sciurus</i>), striped grunt (<i>Haemulon striatum</i>), sailor's grunt (<i>Haemulon parra</i>), porkfish (<i>Anisotremus virginicus</i>), neon goby (<i>Gobiosoma oceanops</i>)
Reef omnivores	HTL	Doctorfish (<i>Acanthurus chirurgus</i>), blue tang (<i>Acanthurus coeruleus</i>), blue angelfish (<i>Holacanthus bermudensis</i>), gray angelfish (<i>Pomacanthus arcuatus</i>), cherubfish (<i>Centropyge argi</i>), rock beauty (<i>Holacanthus tricolor</i>), cocoa damselfish (<i>Pomacentrus variabilis</i>), bicolor damselfish (<i>Pomacentrus partitus</i>), beau gregory (<i>Pomacentrus leocostictus</i>), yellowtail damselfish (<i>Microspathodon chrysurus</i>), seaweed blenny (<i>Parablennius marmoreus</i>), striped parrotfish (<i>Scarus croicensis</i>), bridled goby (<i>Coryphopterus glaucofraenum</i>), Bermuda chub (<i>Kyphossus sectarix</i>), combtooth blenny (<i>Chasmodes saburrae</i>), banded blenny (<i>Paraclinus fasciatus</i>), blenny (<i>Ophioblennius atlanticus</i>), barred blenny (<i>Hypleurochilus bermudensis</i>), sailfin blenny (<i>Emblemaria pandionis</i>), glass blenny (<i>Coralliozetus diaphanus</i>), saddled blenny (<i>Malacoctenus triangulatus</i>), hairy blenny (<i>Labrisomus nuchipinnis</i>), wrasse blenny (<i>Hemiemblemaria simulus</i>), twospot cardinalfish (<i>Apogon maculatus</i>), sponge cardinalfish (<i>Phaeoptyx xenus</i>), purple reefish (<i>Chromis scotti</i>), yellowtail reefish (<i>Chromis enchrysurus</i>), blue chromis (<i>Chromis cyanea</i>), jawfish (<i>Opistognathus aurifrons</i>), dusky jawfish (<i>Opistognathus whitehursti</i>), moustache jawfish (<i>Opistognathus lonchurus</i>), banded jawfish (<i>Opistognathus macrognathus</i>), jawfish (<i>Opistognathus nothus</i>), ocean surgeon (<i>Acanthurus bahianus</i>), banded butterfly (<i>Chaetodon striatus</i>), bank butterfly (<i>Chaetodon aya</i>), foureye butterfly (<i>Chaetodon</i>

		<i>capriistratus</i>), longnose butterfly (<i>Chaetodon aculeatus</i>), reef butterfly (<i>Chaetodon sedentarius</i>), spotfin butterfly (<i>Chaetodon ocellatus</i>), French angel (<i>Pomacanthus paru</i>), queen angel (<i>Holacanthus ciliaris</i>), blue reef damsel (<i>Chromis cyaneus</i>), brown reef damsel (<i>Chromis multilineata</i>), orange damsel (<i>Pomacentrus planifrons</i>), scarletback damsel (<i>Pomacentrus fuscus</i>), sergeant major damsel (<i>Abudefduf saxatilis</i>), sunshine damsel (<i>Chromis insolatus</i>), longfin damselfish (<i>Pomacentrus diencaeus</i>), blue parrot (<i>Scarus coeruleus</i>), queen parrot (<i>Scarus vetula</i>), rainbow parrot (<i>Scarus guacamaia</i>), redband parrot (<i>Sparisoma aurofrenatum</i>), spotlight parrot (<i>Sparisoma viride</i>), midnight parrotfish (<i>Scarus coelestinus</i>), princess parrotfish (<i>Scarus taeniopterus</i>), Gulf surgeonfish (<i>Acanthurus randalli</i>), yellow chub (<i>Kyphosus incisor</i>), redband parrotfish (<i>Sparisoma chrysopterus</i>), bucktooth parrotfish (<i>Sparisoma radians</i>), redband parrotfish (<i>Sparisoma rubripinne</i>)
Shrimps	HTL	Pink shrimp (<i>Farfantepenaeus duorarum</i>), white shrimp (<i>Litopenaeus setiferus</i>), mantis shrimp (<i>Squilla empusa</i>)
Large crabs	HTL	Blue crab (<i>Callinectes sapidus</i>), stone crabs (<i>Menippe mercenaria</i> and <i>Menippe adina</i>), horseshoe crab (<i>Limulus polyphemus</i>), hermits crabs (<i>Pylopagurus operculatus</i> and <i>Clibanaris vittatus</i>), spider crab (<i>Stenocionops furcatus</i>), arrow crab (<i>Stenorynchus seticornis</i>)
Meiofauna	LTL	Harpacticoida spp., Kinorhyncha spp., Nematoda spp., Halacaridae spp., Nauplii spp., Cyclopoida spp., Gastrotricha spp., Acari spp., Tartigrada spp., Rotifera spp., Loricifera spp.
Small infauna	LTL	Aplacophora spp., Cumacea spp., Polychaeta spp.
Small mobile epifauna	LTL	Amphipoda spp., Isopoda spp., Mysidacea spp., Ostracoda spp., Tanaidacea spp., Turbellaria spp., Leptostraca spp., Cladocera spp.
Bivalves	LTL	Bivalvia spp.
Echinoderms and gastropods	LTL	Asteroida spp., Echinoidea spp., Gastropoda spp., Holothuroidea spp.
Zooplankton	LTL	Small phytoplankton, diatoms
Phytoplankton	LTL	Small copepods, large mesozooplankton

883 **Table 2.** Datasets included in the comprehensive survey database for the Gulf of Mexico
884 (GOM). Details about the datasets can be found in Supplementary Table S1.

Name of the survey	Alias	Fisheries-independent or fisheries-dependent survey?	Quality of the survey	Why considered to be of high or low quality?
Alabama Marine Resources Division (AMRD) Fisheries Assessment and Monitoring Program (FAMP) Gillnet Survey	ALGILL	Fisheries-independent	High quality	Has a high spatio-temporal resolution
National Marine Fisheries Service (NMFS) Bottom Longline Survey	BLL	Fisheries-independent	High quality	Has a high spatio-temporal resolution
Deep Pelagic Nekton Dynamics of the Gulf of Mexico (DEEPEND) Survey	DEEPEND	Fisheries-independent	Low quality	Has a low spatio-temporal resolution; the data available to us were collected at a limited number of sites over two months of two consecutive years (May and August) in the offshore areas of north-central GOM only
Northern GOM Continental Slope Habitats and Benthic Ecology Study (DGoMB) Survey	DGOMB	Fisheries-independent	Low quality	Has a low spatio-temporal resolution; collected data at a limited number of sites during the summer months of the period 2000-2002 in the offshore areas of the GOM only
NMFS Expanded Annual Stock Assessment (EASA) Survey – Longline	EASALL	Fisheries-independent	High quality	Has a high spatial resolution
NMFS EASA Survey – Vertical Line	EASAVL	Fisheries-independent	High quality	Has a high spatial resolution
Fish and Wildlife Research Institute (FWRI) Bay Seine Survey	FLBAY	Fisheries-independent	High quality	Has a high spatio-temporal resolution
FWRI Haul Seine Survey	FLHAUL	Fisheries-independent	High quality	Has a high spatio-temporal resolution
FWRI For-Hire At-Sea Observer Program	FLOBS	Fisheries-dependent	High quality	Has a high spatio-temporal resolution
FWRI Purse Seine Survey	FLPURSE	Fisheries-independent	High quality	Has a high spatio-temporal resolution
FWRI Reef Fish Trap Survey	FLTRAP	Fisheries-independent	High quality	Has a high spatio-temporal resolution
FWRI Trawl Survey	FLTRAWL	Fisheries-independent	High quality	Has a high spatio-temporal resolution
FWRI Reef Fish Video Survey	FLVIDEO	Fisheries-independent	High quality	Has a high spatio-temporal resolution
Gulf of Mexico Fisheries Information Network (GulFFIN) Head Boat Port Sampling Program	GULFFINPORT	Fisheries-dependent	Low quality	Has a high spatial resolution; however, the geographic coordinates associated with some of the GULFFINPORT data are located inland (due to fishers unwilling to share the geographic coordinates of their fishing locations)
NMFS Gulf of Mexico Shark Popping and Nursery (GULFSPAN) Survey	GULFSPAN	Fisheries-independent	High quality	Has a high spatio-temporal resolution
Southeast Area Monitoring and Assessment Program (SEAMAP) Gulf of	INBLL	Fisheries-independent	High quality	Has a high spatio-temporal resolution

Mexico Inshore Bottom Longline Survey				
Louisiana Department of Wildlife and Fisheries (LDWF) Vertical Line Survey	LAVL	Fisheries-independent	High quality	Has a high spatio-temporal resolution
Mississippi Department of Marine Resources (MDMR) Sport Fish Shark Gillnet Survey	MSGILL	Fisheries-independent	Low quality	Has a high spatio-temporal resolution; however, teleosts were documented by number caught in each panel in later years only
MDMR Sport Fish Shark Handline Survey	MSHAND	Fisheries-independent	High quality	Has a high spatio-temporal resolution
MDMR Fisheries Assessment and Monitoring (FAM) Trawl Survey	MSTRAWL	Fisheries-independent	High quality	Has a high spatio-temporal resolution
NMFS Southeast Gillnet Observer Program	OBSGILL	Fisheries-dependent	Low quality	Has a high spatio-temporal resolution; however, some of the OBSGILL data were collected in very close proximity (using different panels of the same gear)
Reef Fish Bottom Longline Observer Program	OBSLL	Fisheries-dependent	High quality	Has a high spatio-temporal resolution
Southeastern Shrimp Fisheries Observer Coverage Program	OBSSHRIMP	Fisheries-dependent	High quality	Has a high spatio-temporal resolution
Reef Fish Vertical Line Observer Program	OBSVL	Fisheries-dependent	High quality	Has a high spatio-temporal resolution
NMFS Panama City Trap Survey	PCTRAP	Fisheries-independent	High quality	Has a high spatio-temporal resolution
NMFS Panama City Video Survey	PCVIDEO	Fisheries-independent	High quality	Has a high spatio-temporal resolution
NMFS Pelagic Observer Program	POP	Fisheries-dependent	High quality	Has a high spatio-temporal resolution
Reef Environmental Education Foundation (REEF) Fish Survey Project	REEF	Fisheries-independent	High quality	Has a high spatio-temporal resolution
NMFS Shark Bottom Longline Observer Program	SBLOP	Fisheries-dependent	High quality	Has a high spatio-temporal resolution
NMFS Small Pelagics Survey	SMALLPEL	Fisheries-independent	High quality	Has a high spatio-temporal resolution
SEAMAP Groundfish/Trawl Survey	TRAWL	Fisheries-independent	High quality	Has a high spatio-temporal resolution
Texas Parks and Wildlife Department (TPWD) Bottom Longline Survey	TXBLL	Fisheries-independent	High quality	Has a high spatio-temporal resolution
TPWD Gillnet Survey	TXGILL	Fisheries-independent	High quality	Has a high spatio-temporal resolution
TPWD Seine Survey	TXSEINE	Fisheries-independent	High quality	Has a high spatio-temporal resolution
TPWD Trawl Survey	TXTRAWL	Fisheries-independent	High quality	Has a high spatio-temporal resolution
SEAMAP Reef Fish Video Survey	VIDEO	Fisheries-independent	High quality	Has a high spatio-temporal resolution
SEAMAP Gulf of Mexico Vertical Longline Survey	VL	Fisheries-independent	High quality	Has a high spatio-temporal resolution

886 **Table 3.** Number of encounters and regional percentages of younger juveniles (ages 0-1)
887 of red snapper (*Lutjanus campechanus*), red grouper (*Epinephelus morio*) and gag
888 (*Mycteroperca microlepis*) collected within the U.S. Gulf of Mexico by fisheries-
889 independent surveys and observer programs that use random sampling schemes. Datasets
890 are as defined in Table 2. % East = percentage of encounters east of 87°W (i.e., percentage
891 of encounters on the West Florida Shelf).

Fish life stage	Dataset	Number of encounters	% East
Younger juvenile red snapper	EASAVL	3	0
	FLOBS	7	100
	FLTRAP	3	33.3
	OBSSHRIMP	12,270	7.9
	OBSVL	19	19
	PCTRAP	8	100
	SBLOP	4	100
	SMALLPEL	166	1.2
	TRAWL	4,144	3.5
	TXTRAWL	1,480	0
	VIDEO	7	42.9
	VL	10	0
Younger juvenile red grouper	FLBAY	2	100
	FLHAUL	29	100
	FLOBS	1	100
	FLTRAWL	59	100
	SBLOP	4	100
	TRAWL	44	100
Younger juvenile gag	FLBAY	87	100
	FLHAUL	532	100
	FLPURSE	28	100
	FLTRAWL	348	100

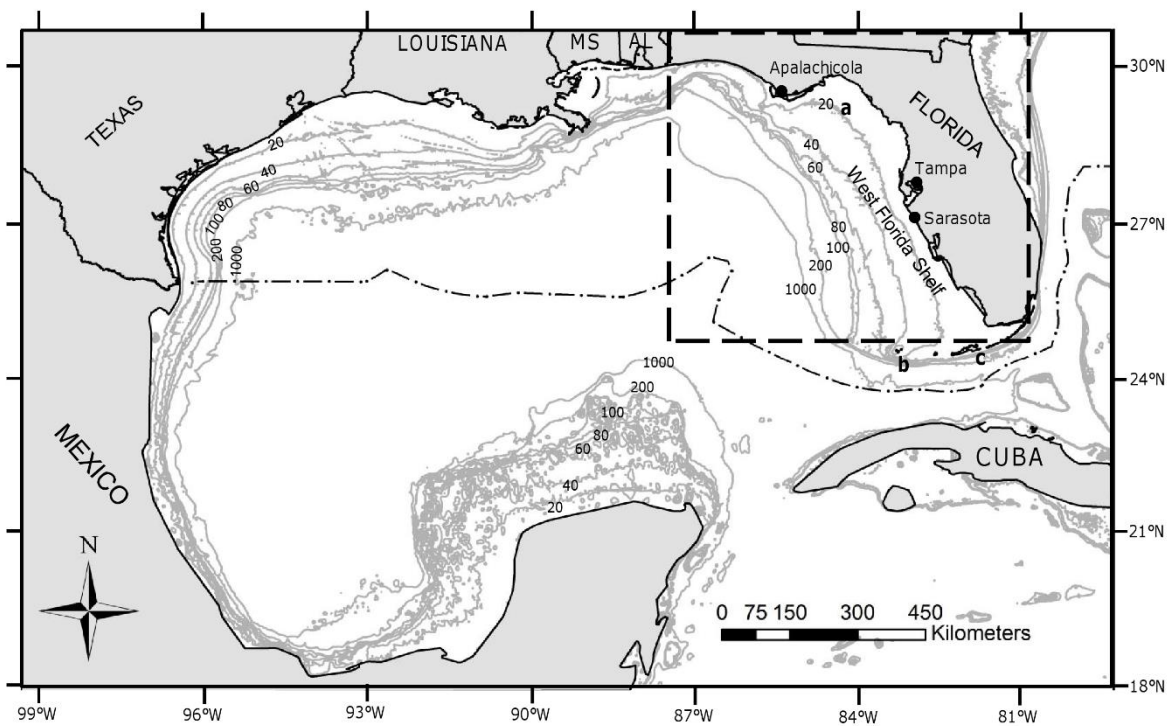
892 **Table 4.** Percentages of spatial overlap between younger juveniles (ages 0-1) of red
 893 snapper (*Lutjanus campechanus*), red grouper (*Epinephelus morio*) and gag (*Mycteroperca*
 894 *microlepis*) and older juveniles (ages 1-3) and adults (ages 3+) of red grouper and gag.

895

Younger juvenile life stage	Older juvenile or adult life stage	Percentage of spatial overlap
Younger juvenile red snapper	Older juvenile red grouper	36%
	Adult red grouper	70%
	Older juvenile gag	21%
	Adult gag	26%
Younger juvenile red grouper	Older juvenile red grouper	78%
	Adult red grouper	81%
	Older juvenile gag	19%
	Adult gag	8%
Younger juvenile gag	Older juvenile red grouper	42%
	Adult red grouper	25%
	Older juvenile gag	72%
	Adult gag	14%

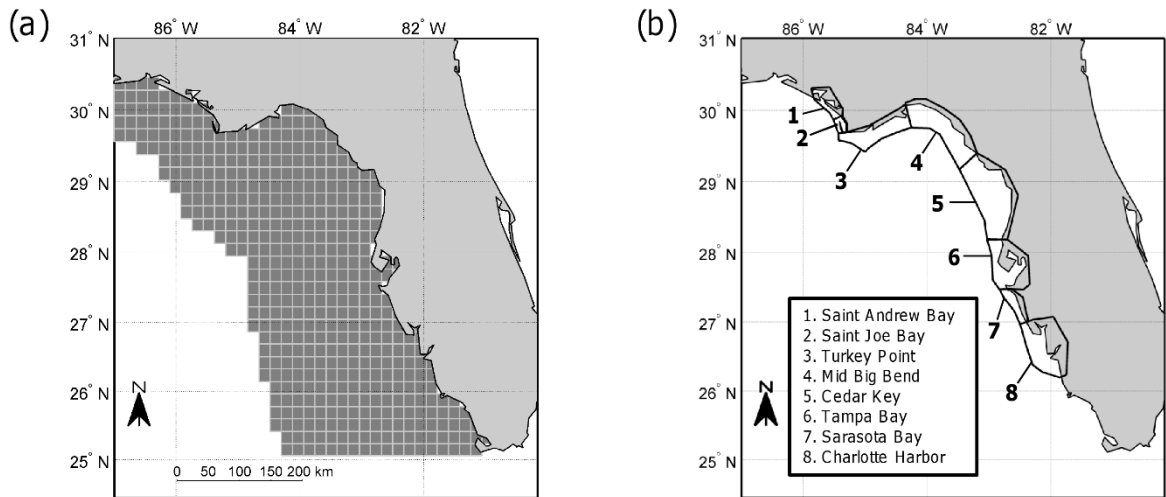
896 **Figure captions**

897 **Figure 1.** Map of the Gulf of Mexico. Depth contours are labeled in 20-, 40-, 60-, 80-,
898 100-, 200-, and 1000-m contours. Important features are labeled and include: the West
899 Florida Shelf, the Apalachee Bay (a), Dry Tortugas (b), and the Florida Keys (c). MS =
900 Mississippi - AL = Alabama. The black dashed-dotted line delineates the U.S. exclusive
901 economic zone, while the black dashed rectangle delineates the spatial domain of the
902 OSMOSE-WFS ecosystem model.



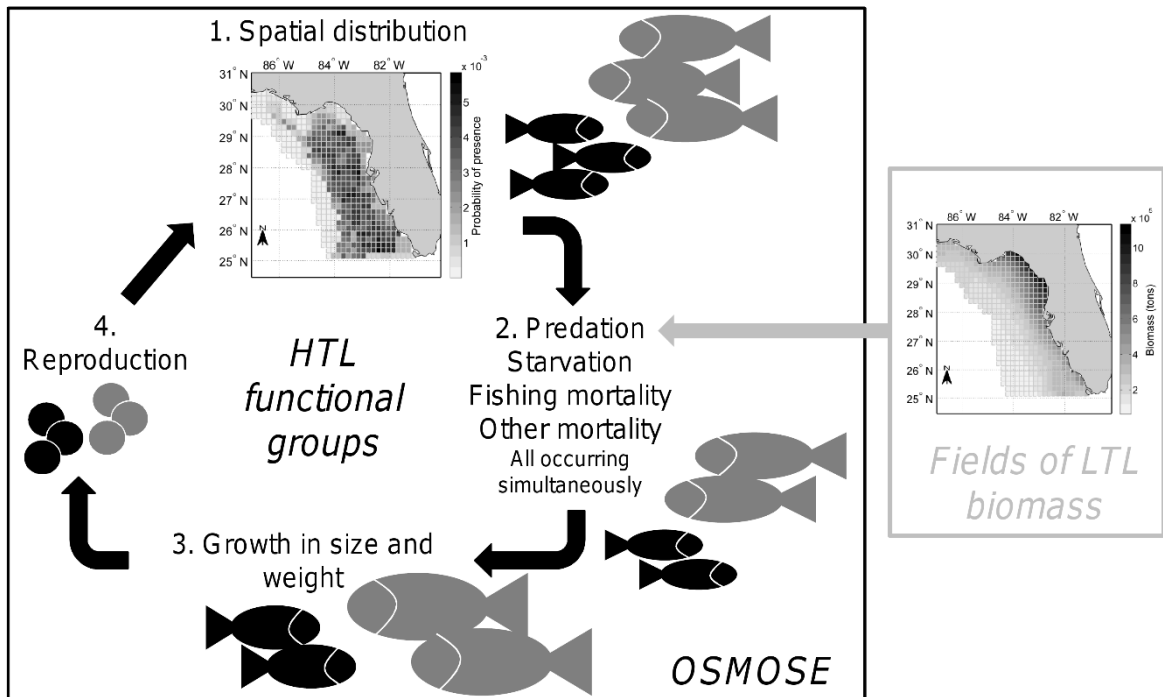
903

904 **Figure 2.** Maps of the West Florida Shelf in the Gulf of Mexico showing: **(a)** the spatial
905 cells of the OSMOSE-WFS ecosystem model (filled in dark grey); and **(b)** the regions
906 where younger juveniles (ages 0-1) of gag (*Mycteroperca microlepis*) have been
907 consistently found over the recent years (Ingram *et al.*, 2013).



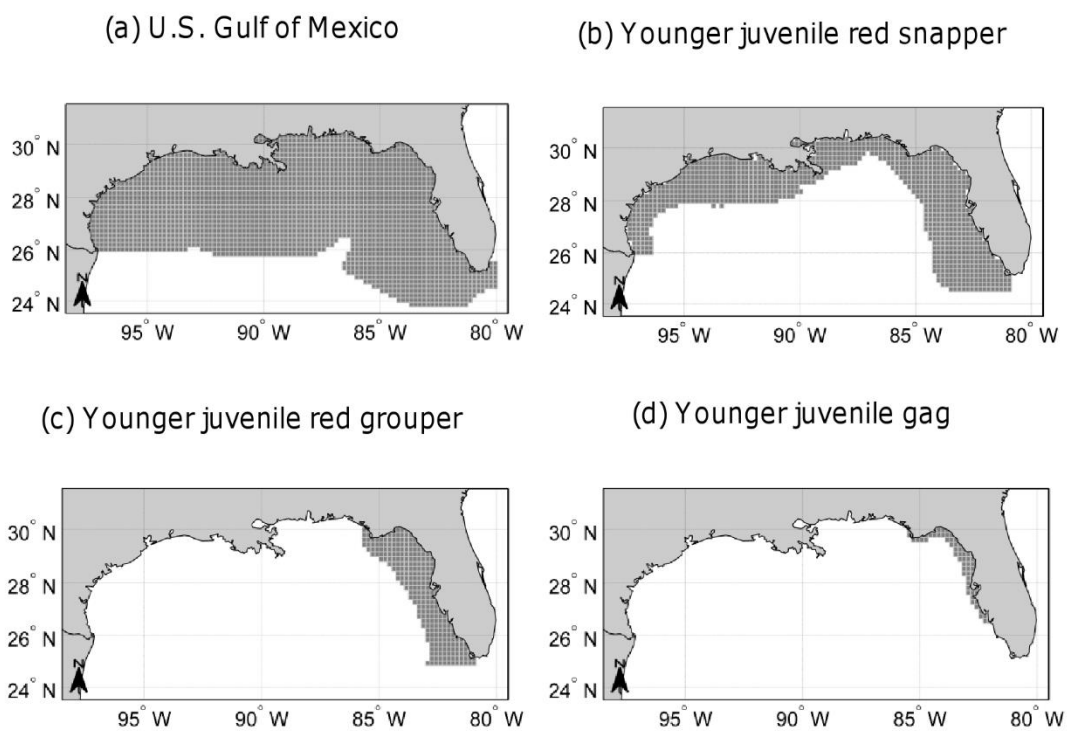
908

909 **Figure 3.** Succession of events within each monthly time step in the OSMOSE-WFS
 910 ecosystem model. The OSMOSE-WFS model simulates the entire life cycle of 12 high
 911 trophic level (HTL) functional groups and is forced by fields of biomass for nine low
 912 trophic level (LTL) functional groups; fields of LTL biomass only serve to provide
 913 additional food to the modelled system.



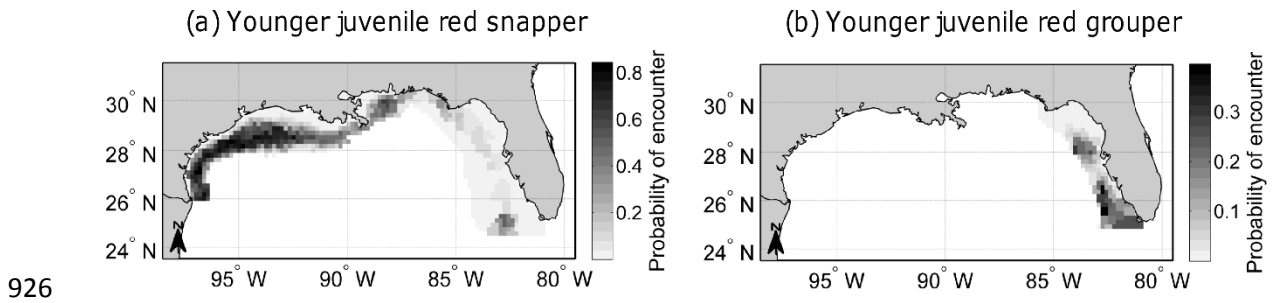
914

915 **Figure 4.** Spatial grids constructed for the present study. **(a)** $0.18^{\circ} \times 0.18^{\circ}$ spatial grid for
916 the U.S. Gulf of Mexico. **(b-d)** Spatial prediction grids defined for **(b)** younger juvenile
917 (ages 0-1) red snapper (*Lutjanus campechanus*); **(c)** younger juvenile (ages 0-1) red
918 grouper (*Epinephelus morio*); and **(d)** younger juvenile (ages 0-1) gag (*Mycteroperca*
919 *microlepis*). The extent of the prediction grid of a given fish life stage was defined from
920 the spatial grid for the U.S. GOM, based on the ranges of latitude, longitude and bottom
921 depth at which this life stage occurs according to survey data.



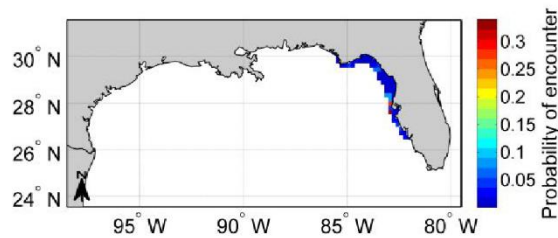
922

923 **Figure 5.** Distribution maps produced from the predictions of spatio-temporal generalized
924 linear mixed models for **(a)** younger juvenile (ages 0-1) red snapper (*Lutjanus*
925 *campechanus*); and **(b)** younger juvenile (ages 0-1) red grouper (*Epinephelus morio*).

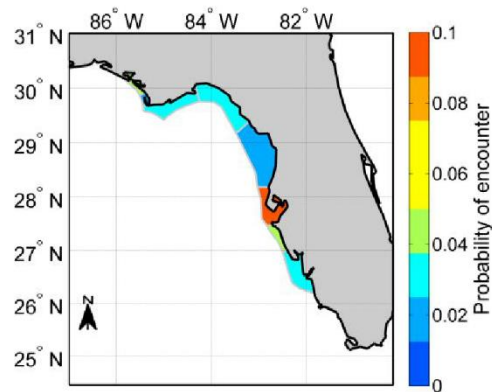


927 **Figure 6.** Distribution maps produced from the predictions of a spatio-temporal
928 generalized linear mixed model for younger juvenile (ages 0-1) gag (*Mycteroperca*
929 *microlepis*). **(a)** is a probability of encounter map for the entire U.S. Gulf of Mexico. **(b)**
930 shows the average probability of encounter of younger juvenile gag in the eight regions of
931 the West Florida Shelf where the life stage has been consistently found over the recent
932 years (Ingram *et al.*, 2013).

(a)



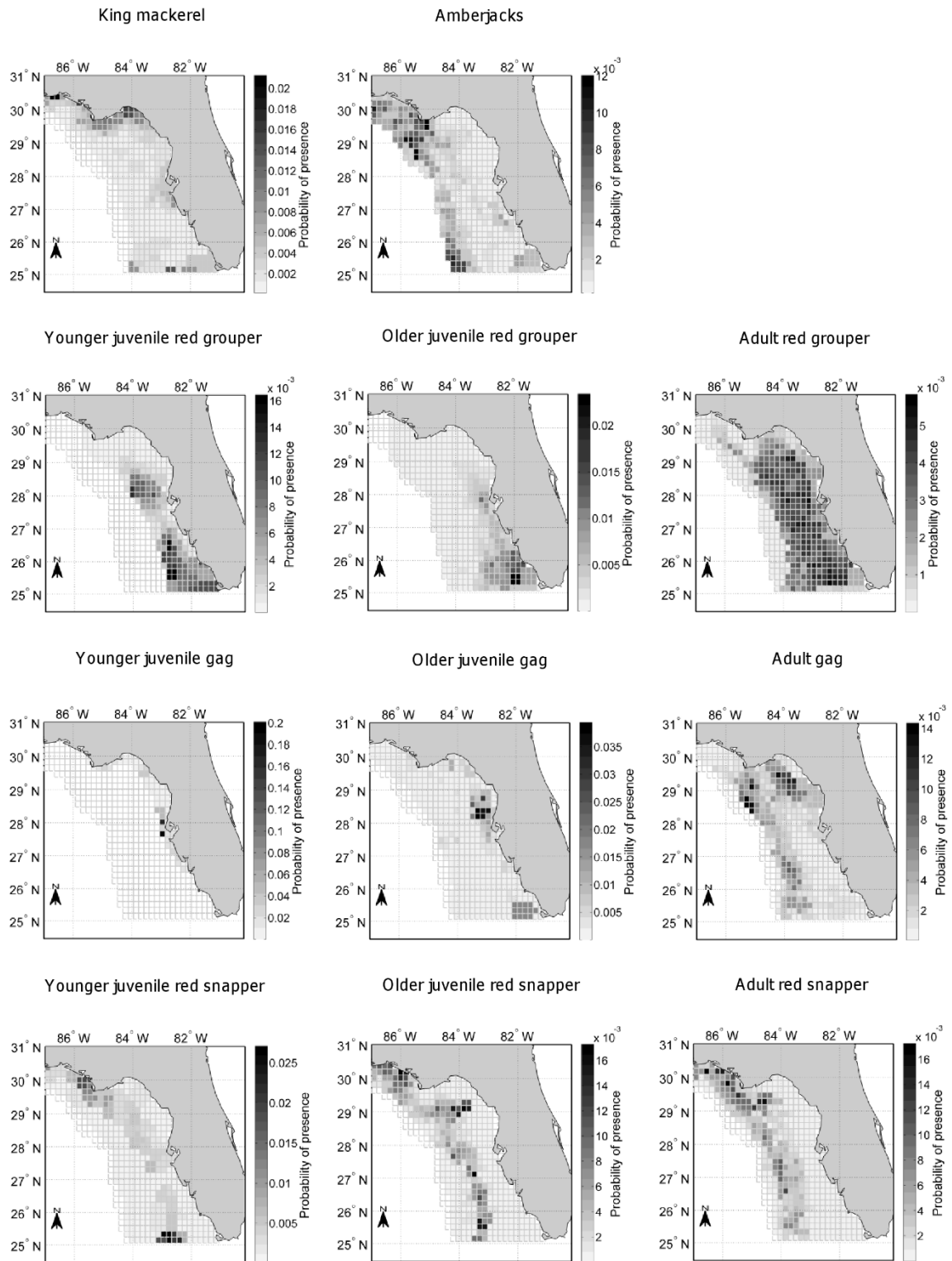
(b)



933

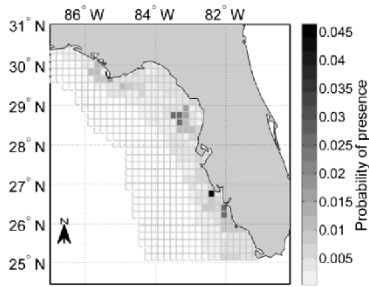
934 **Figure 7.** Distribution maps produced for the functional groups and life stages represented
 935 in the OSMOSE-WFS ecosystem model.

936

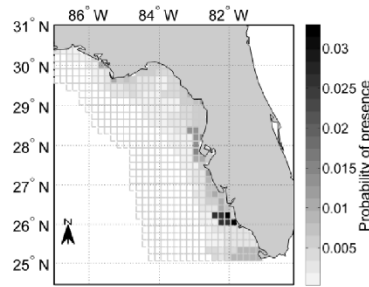


937

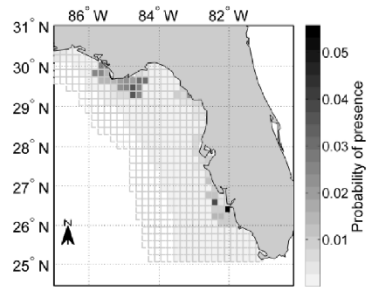
Sardine-herring-scad-complex in spring-summer



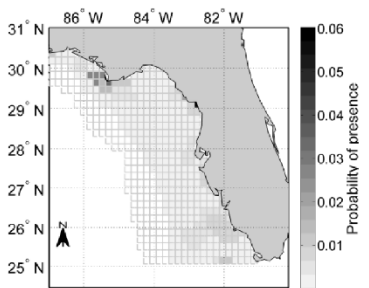
Sardine-herring-scad complex in fall-winter



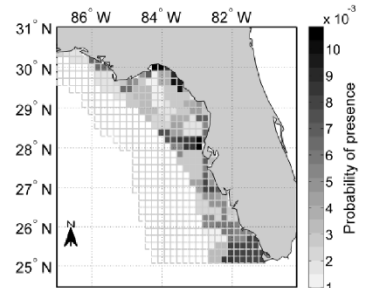
Anchovies-silversides in winter-spring



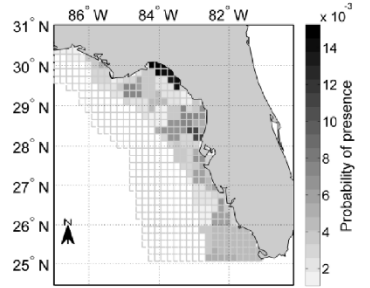
Anchovies-silversides in summer-fall



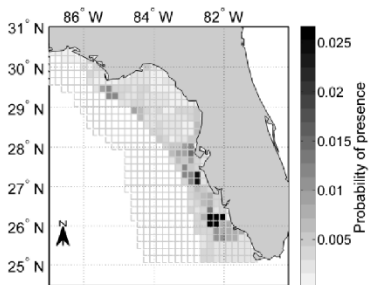
Juvenile coastal omnivores in spring-summer



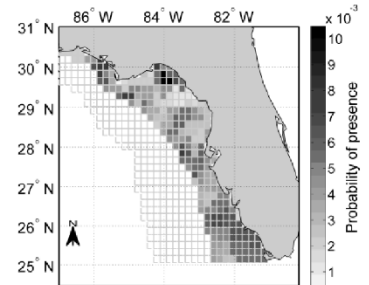
Juvenile coastal omnivores in fall-winter



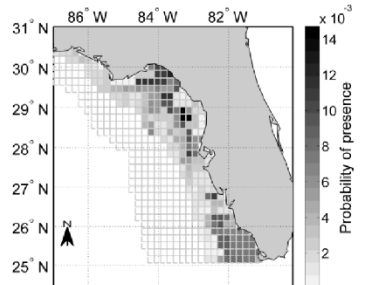
Adult coastal omnivores in spring-summer



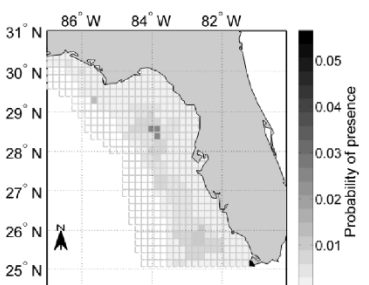
Adult coastal omnivores in fall-winter



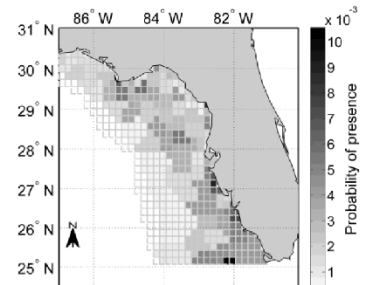
Reef carnivores



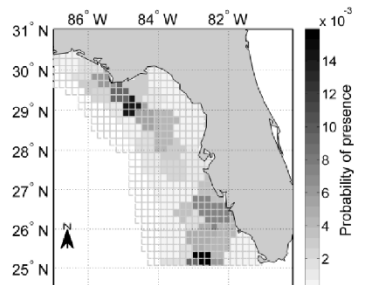
Reef omnivores



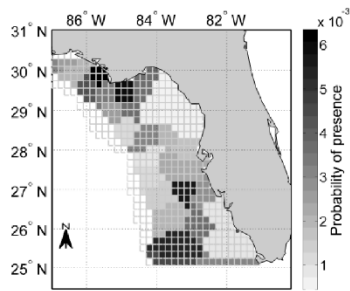
Juvenile shrimps



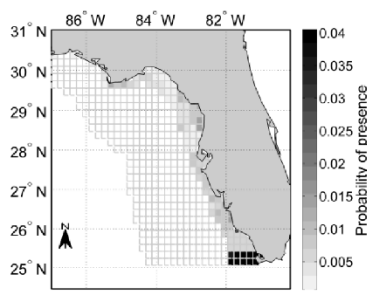
Adult shrimps in spring-summer



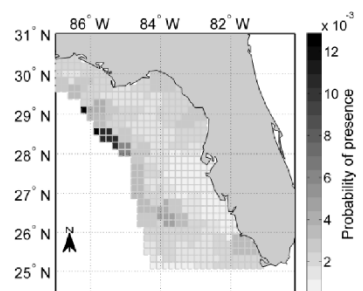
Adult shrimps in fall-winter



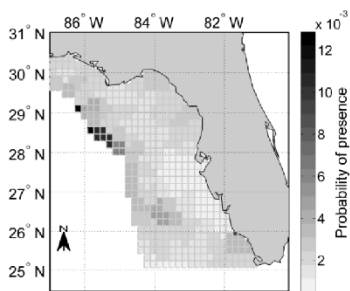
Large crabs



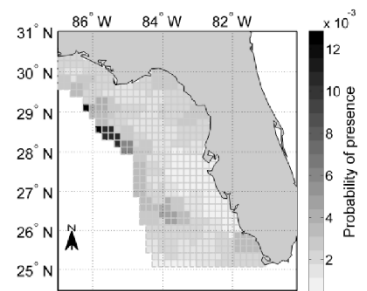
Meiofauna



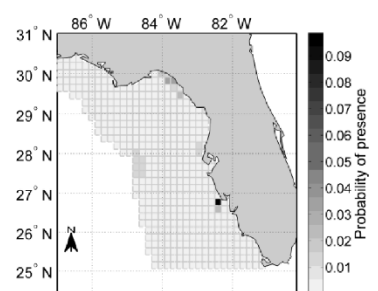
Small infauna



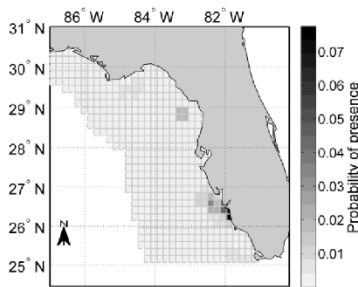
Small mobile epifauna



Bivalves



Echinoderms and gastropods



941 **Boxes**

942 **Box 1. Discussion of the spatial distribution patterns of younger juveniles of red**
943 **snapper, red grouper and gag predicted in the present study.**

944 The comprehensive survey database for the Gulf of Mexico (GOM) provided a
945 large amount of encounter data for younger juvenile red snapper. In the case of younger
946 juvenile red snapper, data collected over the entire U.S. GOM shelf (by OBSSHRIMP,
947 SMALLPEL and TRAWL) and over the Texas continental shelf (by TXTRAWL) were
948 retained in the comprehensive survey database. The great majority of younger juvenile red
949 snappers collected by these surveys were encountered in the western U.S. GOM (Table 3)
950 and, therefore, the spatio-temporal binomial generalized linear mixed model (GLMM) of
951 younger juvenile red snapper predicted the probability of encounter of the fish life stage to
952 be much higher in the western U.S. GOM than in the eastern U.S. GOM (i.e., than on the
953 West Florida Shelf) (Figure 5a). The literature on the spatial distribution of younger
954 juvenile red snapper is limited, due to the cryptic nature of the fish life stage (Szedlmayer
955 and Mudrak, 2014). However, the rare studies on the spatial distribution of younger
956 juvenile red snapper also report that the bulk of younger juvenile red snappers are found
957 from the Florida-Alabama border to the Texas-Mexico border (Gallaway *et al.*, 1999,
958 2009; Monk *et al.*, 2015).

959 The spatial distribution patterns of younger juvenile red snapper predicted in the
960 present study concur with the limited literature on the topic. Firstly, we found that hotspots
961 of probability of encounter for younger juvenile red snapper are located in those areas of
962 the GOM where bottom depth ranges from 20 to 60 m, while Johnson *et al.* (2013)
963 reported that high-value red snapper larval settlement habitat occurs between 15 and 64 m
964 of water depth. Gallaway *et al.* (1999) estimated that younger juvenile red snapper habitat
965 lies in areas of the GOM where bottom depth ranges from 18 and 64 m and the authors

966 found peak abundance for the life stage at 37 m of water depth, while we predicted
967 younger juvenile red snapper to be encountered at 43 m of water depth on average.
968 Secondly, consistent with Szedlmayer and Conti (1999) and Gallaway *et al.* (1999), we
969 found that the greatest probabilities of encounter of younger juvenile red snapper in the
970 western U.S. GOM are located in the mid-shelf area offshore Alabama and on the Texas
971 continental shelf. Finally, the spatio-temporal binomial GLMM of younger juvenile red
972 snapper predicted the probability of encounter of the life stage in the eastern U.S. GOM to
973 be highest near the Florida Keys and Dry Tortugas, which concurs with Karnauskas *et al.*
974 (2013a); Karnauskas *et al.* (2013a) carried out simulations with the Connectivity
975 Modelling System (CMS) biophysical model, which revealed that red snapper larval
976 settlement on the West Florida Shelf is poor and primarily occurs in the southern extent of
977 the Shelf. Our results could be used to improve understanding of where younger juvenile
978 red snappers are likely to be caught as bycatch in shrimp trawls (Monk *et al.*, 2015).

979 Despite the compilation of a comprehensive survey database for the GOM, we had
980 limited encounter data for younger juvenile red grouper (Table 3). This result is due to the
981 cryptic nature of red grouper, which has not allowed previous studies to determine the
982 dominant habitat of the younger juveniles of the species (Moe, 1969; Koenig and Coleman,
983 1999; Coleman *et al.*, 2010). In the case of younger juvenile red grouper, fisheries-
984 independent data collected in West Florida waters (by FLTRAWL and FLHAUL) and over
985 the entire U.S. GOM shelf (by TRAWL) suggest that the life stage is distributed on the
986 West Florida Shelf only. The spatio-temporal binomial model of younger juvenile red
987 grouper predicts the life stage to be distributed mainly from Sarasota to the southern West
988 Florida Shelf, at 24 m water depth on average.

989 More encounter data were available for younger juvenile gag than for younger
990 juvenile red grouper (Table 3). In the case of younger juvenile gag, only fisheries-

991 independent datasets for Florida (the FLHAUL, FLTRAWL and FLBAY datasets) were
992 retained in the comprehensive survey database for the GOM. However, younger juvenile
993 gag does not occur solely in West Florida waters. When we contacted the Texas Parks and
994 Wildlife Department to request their survey data, the state agency provided us with the
995 Texas Marine Sport-Harvest Monitoring Program Survey (TXFD) dataset, which reports
996 catches per unit effort (CPUEs) at fixed locations. We extracted encounter/non-encounter
997 data from the TXFD dataset, and found that younger juvenile gag was encountered in
998 Texas coastal waters in 2000. Moreover, since older juveniles and adults of gag are
999 encountered in the western U.S. GOM, we suspect that the younger juveniles of the species
1000 can also be encountered there. Currently, besides the TXFD survey, no research survey in
1001 the western U.S. GOM (conducted using a random or a fixed-station sampling scheme) has
1002 collected data for younger juvenile gag. Therefore, it would be interesting to initiate new
1003 research surveys or to expand existing ones so as to elucidate where younger juvenile gag
1004 is distributed in the western U.S. GOM.

1005 Besides the FLHAUL, FLTRAWL and FLBAY datasets, we received two datasets
1006 that provide a reasonable amount of CPUE data for younger juvenile gag for the West
1007 Florida Shelf: (1) the NMFS Panama City Laboratory St. Andrew Bay Juvenile Reef Fish
1008 Survey (PCJUV), which collects data for gag and a few other species in St. Andrew Bay, at
1009 fixed seagrass locations pre-determined to be settlement areas; and (2) the Florida State
1010 University Estuarine Gag Survey (FSUEST), which collects data for gag at fixed locations,
1011 primarily in seagrass habitat, in the eight regions of the West Florida Shelf where Ingram
1012 *et al.* (2013) reported younger juvenile gag to be consistently found. However, we were
1013 unable to include PCJUV and FSUEST data in the comprehensive survey database for the
1014 GOM, due to the fact that these data were collected using a fixed-station sampling scheme.
1015 Yet, using FLHAUL, FLTRAWL and FLBAY data only, the spatio-temporal binomial

1016 GLMM of younger juvenile gag was able to predict that the life stage is encountered in the
1017 eight regions identified by Ingram *et al.* (2013), namely Saint Andrew Bay, Saint Joe Bay,
1018 Turkey Point, the Mid Big Bend, Cedar Key, Tampa Bay, Sarasota Bay, and Charlotte
1019 Harbor (Figure 6). The spatio-temporal binomial GLMM of younger juvenile gag did not
1020 predict the life stage to occur in the Marco Island region, which is located just south of
1021 Charlotte Harbor (Figure 6b). Ingram *et al.* (2013) excluded the Marco Island region from
1022 their analyses, because, over the period 1991-2012, only a few younger juvenile gags were
1023 caught in the region in 2005, 2006 and 2007. Fitzhugh *et al.* (2005) reported that sampling
1024 to collect younger juvenile gags are usually not conducted in the Marco Island region,
1025 because the great majority of the seagrass beds in that region, which provide suitable
1026 settlement habitat for gag larvae, have been severely reduced since the late 1980s. Experts
1027 report that most of the younger juvenile gags are caught between 0 and 2 m of water depth
1028 (Ingram *et al.*, 2013), while the spatio-temporal binomial GLMM that we fit for younger
1029 juvenile gag predicts the life stage to be encountered at a mean bottom depth of 8 m.

1030 The probabilities of encounter of younger juvenile gag predicted for the eight
1031 regions identified in Ingram *et al.* (2013) are usually consistent with the findings of
1032 previous studies (Switzer *et al.*, 2012, 2015). In accordance with Switzer *et al.* (2012), we
1033 found the probability of encounter of younger juvenile gag to be low in Cedar Key. Switzer
1034 *et al.* (2012) advanced several possible explanations for this. One of these possible
1035 explanations is that discharge from a nearby river (the Suwannee River) is highly variable
1036 and that it diminishes the quality of younger juvenile gag habitat. Another possible
1037 explanation is that gags settling in Cedar Key may be diluted by the large amount of
1038 seagrass habitat in that region, or they may settle at the edge of seagrass habitat in waters
1039 deeper than those at which the FLHAUL, FLTRAWL and FLBAY surveys take place.
1040 Finally, the specific hydrographic conditions in Cedar Key, which is an open coastal

1041 system and not a semi-enclosed estuary (like Tampa Bay, for example), may limit gag
1042 larval settlement in the Cedar Key region (Switzer *et al.*, 2012). Moreover, both the present
1043 study and Switzer *et al.* (2015) found that the probability of encounter of younger juvenile
1044 gag is low in the Mid Big Bend. According to Switzer *et al.* (2015), this may be due in part
1045 to the fact that seagrass habitat is found in deeper waters in the Mid Big Bend than
1046 elsewhere on the West Florida Shelf, and to the fact that drift algae, which reduce the
1047 catchability of younger juvenile gag, are abundant in the Mid Big Bend region. Both this
1048 study and Switzer *et al.* (2015) also found that younger juvenile gag has a high probability
1049 of encounter in Tampa Bay, presumably due to the large quantity of fragmented seagrass
1050 habitat in that region. By contrast, the spatio-temporal binomial GLMM of younger
1051 juvenile gag predicted the probability of encounter of the life stage to be almost as low in
1052 Turkey Point and Charlotte Harbor as in Cedar Key (Figure 6b), which does not concur
1053 with Switzer *et al.* (2015). The low probability of encounter of younger juvenile gag in
1054 Turkey Point predicted by the spatio-temporal binomial GLMM may be explained by the
1055 large winter leaf dieback of seagrasses that occurs earlier in winter in northern West
1056 Florida and results in higher mortality rates in younger juvenile gag in northern West
1057 Florida than in southern West Florida (Fitzhugh *et al.*, 2005; Casey *et al.*, 2007; Switzer *et*
1058 *al.*, 2012). Then, the low probability of encounter of younger juvenile gag in Charlotte
1059 Harbor predicted by its spatio-temporal binomial GLMM may be explained by the smaller
1060 quantity of seagrass habitat in Charlotte Harbor compared to Tampa Bay and Sarasota Bay
1061 (Casey *et al.*, 2007; Switzer *et al.*, 2012). Although younger juvenile gags also inhabit
1062 mangroves, oyster reefs, jetties and seawalls (Hastings, 1979; Bullock and Smith, 1991;
1063 Casey *et al.*, 2007), Casey *et al.* (2007) found that younger juvenile gag CPUE is
1064 significantly correlated with the amount of seagrass habitat.